Dysregulated neuroimmune interactions and sustained type I interferon signaling after human immunodeficiency virus type 1 infection of human iPSC derived microglia and cerebral organoids

Andrew J. Boreland[1,2], Alessandro C. Stillitano[1], Hsin-Ching Lin[1], Yara Abbo[1], Ronald P. Hart[3], Peng Jiang[3], Zhiping P. Pang[1,2*], Arnold B. Rabson[1,4*]

[1] Child Health Institute of New Jersey, Rutgers Robert Wood Johnson Medical School, New Brunswick, NJ

[2] Department of Neuroscience, Rutgers Robert Wood Johnson Medical School, New Brunswick, NJ

[3] Department of Cell Biology and Neuroscience, Rutgers University, Piscataway, NJ

[4] Departments of Pharmacology, Pathology & Laboratory Medicine, and Pediatrics, Rutgers Robert Wood Johnson Medical School, New Brunswick, NJ

*Correspondence: zhiping.pang@rutgers.edu and rabsonab@rwjms.rutgers.edu

Highlights of the work:

- HIV-1 productively infects iPSC-derived microglia and triggers inflammatory activation.
- HIV-1 infection of microglia results in sustained type I interferon signaling.
- Microglia infected by HIV-1 incorporate into sliced neocortical organoids with persistent type I interferon signaling and disease risk gene expression.

ABSTRACT

Human immunodeficiency virus type-1 (HIV-1) associated neurocognitive disorder (HAND) affects up to half of HIV-1 positive patients with long term neurological consequences, including dementia. There are no effective therapeutics for HAND because the pathophysiology of HIV-1 induced glial and neuronal functional deficits in humans remains enigmatic. To bridge this knowledge gap, we established a model simulating HIV-1 infection in the central nervous system using human induced pluripotent stem cell (iPSC) derived microglia combined with sliced neocortical organoids. Upon incubation with two replication-competent macrophage-tropic HIV-1 strains (JRFL and YU2), we observed that microglia not only became productively infected but also exhibited inflammatory activation. RNA sequencing revealed a significant and sustained activation of type I interferon signaling pathways. Incorporating microglia into sliced neocortical organoids extended the effects of aberrant type I interferon signaling in a human neural context. Collectively, our results illuminate the role of persistent type I interferon signaling in HIV-1 infected microglial in a human neural model, suggesting its potential significance in the pathogenesis of HAND.

INTRODUCTION

The global burden of human immunodeficiency virus-1 (HIV-1) infection remains profound, with neurocognitive complications manifesting in a significant proportion of infected individuals despite the remarkable success of combined antiretroviral therapy (cART) in reducing morbidity and mortality. Up to 55% of HIV-1 positive people experience neurological complications that may develop into HIV associated neurocognitive disorder (HAND) (Simioni et al. 2010; Sacktor et al. 2016; Eggers et al. 2017; Sacktor 2018). This debilitating disorder manifests across a spectrum of cognitive, motor, affective, and behavioral impairments, which can severely impact the quality of life for affected individuals, emphasizing an urgent need for a better understanding of its underlying mechanisms (Lew et al. 2018; Israel et al. 2019). The etiology and neuropathogenesis of HAND remain enigmatic, as there has been no evidence of neuronal HIV-1 infection. Decades of research suggest that HAND development is caused by a combination of both direct and indirect effects involving viral proteins, inflammatory cytokines and chemokines, and dysregulated neuroimmune interactions (Koenig et al. 1986; Gendelman et al. 1994; Rappaport et al. 1999; González-Scarano and Martín-García 2005; Kraft-Terry, Buch, Fox, and Gendelman 2009; Lindl, Marks, Kolson, and Jordan-Sciutto 2010; Burdo, Lackner, and Williams 2013; Alvarez-Carbonell et al. 2020). Interestingly, clinical symptoms of HAND correlate more closely with cytokine production, neuronal pathology, decreased synaptic density, and increased microglia than with central nervous system (CNS) viral load (Kaul, Garden, and Lipton 2001; Kaul et al. 2005). Currently there is a lack of mechanistic understanding due to a need for better experimental models that can address these questions, especially regarding neuroimmune interactions.

A pivotal component of neuroimmune interactions is the innate immune response, including the production and signaling of interferons, which have recently been implicated in the neuropathology of various neurological diseases [Reviewed in (Hofer and Campbell 2013; McGlasson, Jury, Jackson, and Hunt 2015)]. Interferons and their downstream signaling through

interferon stimulated genes (ISGs) are primarily an innate immune response to viral infection [reviewed in (Platanias 2005)]. However, recent literature suggests a role for dysregulated type I interferon signaling in neurological diseases such as Alzheimer's disease (Roy et al. 2020; Roy et al. 2022), COVID-19 related brain fog (Lee and Shin 2020; Phetsouphanh et al. 2022), aging associated dementia (Baruch et al. 2014), and HIV associated dementia (Rho et al. 1995; Krivine et al. 1999; Perrella et al. 2001; Anderson et al. 2017; Solomon et al. 2020). Clinically, type I interferons have been shown to be a driver of cognitive impairment both in diseased states and when administered exogenously (Merimsky, Reider-Groswasser, Inbar, and Chaitchik 1990). Indeed, many studies using interferon treatment for various severe cancers and chronic viral hepatitis C have reported that patients receiving interferon-alpha displayed cognitive, mood, and behavioral deficits that arose and worsened with prolonged, multiweek treatment regimens (Christina, Randall, and Arthur 1991; Pavol et al. 1995; Capuron, Ravaud, and Dantzer 2001; Capuron et al. 2002; Wichers et al. 2005; Raison, Demetrashvili, Capuron, and Miller 2005). Taken together, these studies indicate a role for aberrant type I interferon signaling in compromising neuronal and glial function, leading to cognitive deficits and degeneration.

Microglia, as the resident immune cells of the CNS and the primary CNS target and reservoir of HIV-1 infection (Tang et al. 2023), contribute significantly to the pathophysiology of HAND, largely through their secretory and functional dysregulation. Under homeostatic conditions, microglia play important roles in synaptic pruning, phagocytic functions, immune surveillance, and extracellular matrix remodeling (Paolicelli et al. 2011; Casano and Peri 2015). When challenged, microglial activation can be either neurotoxic, producing proinflammatory cytokines and chemokines, or neurotrophic, producing anti-inflammatory cytokines (Durafourt et al. 2012). Microglia exhibit a heterogeneous spectrum of activation and disease-associated states with unique properties and consequences on neuronal functions (Gosselin et al. 2017; Song and Colonna 2018; Hammond et al. 2019).

Since HIV-1 specifically infects humans, the ability of traditional animal model organisms to replicate the complex disease processes of HAND is inherently limited. HIV-1-Simian immunodeficiency virus chimeras (SHIVs) have been studied in monkey models. However, these models are limited in their availability and utility for molecular analyses [reviewed in (Byrnes et al. 2022; Moretti et al. 2021)]. Recent advances in stem cell technologies have opened up new possibilities for modeling and studying HAND, particularly the development of human iPSC derived neurons, astrocytes, and microglia capable of mimicking complex in vivo neuroimmune interactions when grown in three dimensional cerebral organoid cultures (Abud et al. 2017; Ormel et al. 2018; Xu et al. 2021). Cerebral organoids offer a powerful and physiologically relevant platform to study complex neuroimmune interactions, but traditional organoid differentiation protocols do not produce microglia [reviewed in(Dos Reis, Sant, and Ayyavoo 2023; Swingler et al. 2023; Wei et al. 2023)]. Recent studies have demonstrated the feasibility of infecting iPSC-derived macrophages (Vaughan-Jackson et al. 2021) and microglia (Rai et al. 2020) with HIV-1. Moreover, these infected microglia have been effectively cocultured in various model systems, including human stem cell derived neural tricultures (Alvarez-Carbonell et al. 2020; Ryan et al. 2020), primary neuron progenitor cell derived organoids (dos Reis et al. 2020), iPSC-derived cerebral organoids (Gumbs et al. 2022), and a humanized mouse model (Min et al. 2023).

In this study, we hypothesized that by infecting iPSC-derived microglia with replication competent HIV-1 and integrating them into sliced neocortical organoids, we could recapitulate neuroimmune dysregulation related to HAND pathology. We demonstrate that HIV-1 infection of iPSC-derived microglia leads to persistent activation of type I interferon signaling and microglial activation in both microglial monocultures and in the context of cerebral organoids.

RESULTS

Human microglia are efficiently generated from iPSCs

To induce microglial differentiation, we used three iPSC lines and employed previous protocols (Haenseler et al. 2017; Xu et al. 2021). To mimic in vivo microglial development from the yolk sac, iPSC embryoid bodies were patterned toward a mesodermal yolk sac lineage that generates primitive macrophage precursors (PMPs) after 3 weeks of culture (**Figure 1A**). The identity of the PMPs was confirmed by immunocytochemistry against CD235, a marker for yolk sac (Claes, Van den Daele, and Verfaillie 2018), and CD43, a marker for hematopoietic progenitor like cells (Vodyanik, Thomson, and Slukvin 2006) (**Figure 1B**). Upon further maturation under the influence of a colony stimulating factor 1 receptor (CSF1R) antagonist, interleukin 34 (IL-34), and granulocyte maturation factor (GM-CSF), PMPs exhibit a more pronounced microglial phenotype. This was evidenced by a significant increase in mRNA expression of the microglial markers ionized calcium binding molecule 1 (IBA1) and purinergic receptor P2Y12 across all three cell lines (**Figure 1C,** biological replicates of each cell line shown in **Figure S1**). Supporting these gene expression results, we noted robust immunocytochemical staining of the microglial markers IBA1, P2Y12, CX3CR1, transmembrane protein 119 (TMEM119), and transcription factor PU.1 in maturing microglia from these same lines (**Figure 1D**). Upon coculture of microglia with iPSC-derived neurons (Xu et al. 2021), we found that microglia display a more elaborate morphology (**Figure 1E**). Furthermore, costaining with the neuronal dendritic marker microtubule-associated protein 2 (MAP2) and the presynaptic marker synapsin 1 (SYN1) revealed that microglial processes interact with dendrites and colocalize with synaptic puncta, indicating putative microglia-synapse interactions (**Figure 1F**).

Given the tropism of HIV-1 for CD4 receptor expressing cells and the requirement of CCR5 coreceptor expression for infection of monocyte/macrophage related cell lineages, we assessed the gene expression of *CD4* and *CCR5* in iPSC-derived microglia. Results showed significantly increased mRNA expression of *CD4* and *CCR5* in microglia differentiated from all

three iPSC lines (**Figure 1G,** biological replicates of each cell line shown in **Figure S1**). These results demonstrate that microglia can be successfully and reproducibly generated from iPSCs. Crucially, these cells express appropriate markers for microglial identity and infection by HIV-1.

iPSC derived microglia are productively infected by HIV-1 and exhibit inflammatory activation

Having confirmed the generation and maturation of iPSC-derived microglia, we next determined whether these cells could sustain a productive infection by replication competent, macrophage tropic HIV-1. To this end, we incubated male 03SF iPSC-derived microglia with JRFL HIV (2 ng/ml), an R5 tropic HIV-1 strain isolated from the cerebral spinal fluid (CSF) of a patient with severe HAND (Koyanagi et al. 1987; Merrill et al. 1992). Compared to uninfected controls, HIV-1-infected microglia robustly expressed HIV-1 *gag/pol* RNA within 6-9 days after infection (Yu et al. 1996) (**Figure 2A**). As a key indicator of productive HIV-1 infection, the production of secreted p24 was measured (Chargelegue and O'Toole 1992; Marodon, Warren, Filomio, and Posnett 1999). Using ELISA to detect secreted p24 in the culture supernatant, we observed increased protein production starting 1 week post infection, peaking around day 16, and then maintaining consistent levels for more than 2 weeks (**Figure 2B**). Finally, we found that after just 4 days post infection, circular polymerase chain reaction (PCR) products from both long terminal repeats (LTR) were detected in HIV-1 incubated cultures indicating the presence of active viral replication (Butler, Hansen, and Bushman 2001) (**Figure S2**).

After establishing the infectability of iPSC microglia with HIV-1 JRFL, we then asked whether HIV-1 infection elicits differential expression of inflammatory and canonical microglial mRNAs using reverse transcription□quantitative PCR (RT-qPCR). In this second experiment found we found HIV-1 infection augmented the expression of the inflammation-associated genes interleukin 1ß (IL1ß, on day 16) and tumor necrosis factor alpha (TNFα), while the

expression of interleukin 6 (IL6) displayed no change (**Figure 2C**). We then examined the mRNA expression of the chemokines CCL2 (monocyte chemoattractant protein 1, MCP-1), CCL3 (macrophage inflammatory protein 1 alpha, MIP-1), and CCL5 (RANTES). These three chemokines play important roles in immune cell recruitment and migration to sites of inflammation and infection and have been found to be elevated in cognitively impaired individuals with HIV-1 (Letendre, Lanier, and McCutchan 1999). A significant elevation in the mRNA expression of CCL2 and CCL3 was observed by day 16 post-infection, whereas the expression of CCL5 remained unchanged (**Figure 2D**). To assess whether microglial identity was altered by HIV-1 infection, we assessed the mRNA expression of the canonical microglial genes IBA1 and P2Y12. While IBA1 remained stable, P2Y12 exhibited significantly increased expression by day 23 post infection (**Figure 2E**). Next, we asked how HIV-1 infection might alter microglial chemokine and cytokine production. Although the levels of most cytokines were below the detection threshold (**Table S1**), we noted a significant surge in the secretion of chemokines M-CSF and interferon inducible protein 10 (IP-10/CXCL10) following HIV-1 infection in the same supernatant used in figure 2B (**Figure 2F**). Finally, to visualize HIV-1 infected cells, we detected HIV-1 p24 protein using a biotin-streptavidin amplification protocol (Eugenin and Berman 2016). On day 13 post infection with JRFL, p24 positive microglia were found (**Figure 2G**). Collectively, our findings suggest that iPSC-derived microglia can sustain an R5 tropic HIV-1 infection and exhibit an inflammatory activation profile consistent with previous studies.

To confirm that HIV-1 JRFL infection of human iPSC-derived microglia resulted in productive infection and inflammatory activation, we chose a female iPSC line, CD06, and infected it with the JRFL strain as well as a second R5 tropic HIV-1 strain, YU2 (Li et al. 1991), isolated from the CSF of a different patient with severe HAND. We confirmed infection by RT-qPCR of viral *gag-pol* RNA, which exhibited significantly increased expression for both strains by day 16 post-infection, with a subsequent decrease (**Figure 3A**). Using ELISA to detect secreted p24 revealed productive infection for both viral strains (**Figure 3B**). We then assessed

the expression of key inflammatory markers and microglial core mRNAs by qPCR. Both JRFL and YU2 infections led to a significant increase in IL1β expression compared to uninfected microglia (**Figure 3C**). Similarly, TNFα was significantly upregulated in the first two weeks of infection but decreased as the productive infection waned (**Figure 3C**). We also observed increased expression of the chemokines CCL2 and CCL3 by days 16 and 23 post infection with both strains (**Figure 3D**). This upregulation then decreased by day 27, correlating with the reduction of productive infection as indicated by the p24 ELISA (**Figure 3A**). In comparison to the unaltered IBA1 expression we found previously, HIV-1 led to a significant reduction in IBA1 expression in CD06 infected microglia (**Figure 3E**). Similar to 03SF infected microglia, CD06 had significant increased expression of P2RY12 (**Figure 3E**). Together, these results demonstrate infectability of human iPSC-derived microglia with multiple, macrophage tropic HIV-1 strains and their ability to elicit an inflammatory response.

Type I interferon stimulated gene expression and sustained activation following HIV-1 infection

To investigate the transcriptional landscape of HIV-1 infected microglia, we performed bulk RNA sequencing on male 03SF iPSC-derived microglia infected by HIV-1 JRFL day 16 post infection. Principal component analysis (PCA) revealed clear separation of the infected vs mock infected samples (**Figure S2**). Differential gene analysis revealed differentially expressed genes (DEGs) including several classic ISGs, such as IFIT3, MX2, ISG15, RSAD2 and others (**Figure 4A**) (**Table S2**). Gene set enrichment analysis (GSEA) confirmed a significant enrichment of genes related to the interferon alpha response (**Table S3**) (**Figure 4B**). Gene ontology analysis identified activation of innate immune responses and several related terms in the biological process component (**Figure 4C, D** and **Figure S3**). The upregulated DEG GO set includes pathways falling into the overall signaling clusters related to interferon signaling and positive regulation of antiviral biotic, interferon alpha/beta, defense against virus, cytokine mediated and

interferon mediated pathways, and negative regulation of viral processes. Among the downregulated DEG GO clusters are pathways related to positive regulation of antigen processing, extracellular organization, granulocyte/leukocyte migration, chemokine-mediated signaling, and spindle assembly checkpoints. Importantly, HIV-1 infection was found to lead to significant induction of many ISGs, including ISG15, IRF7, MX1, OAS1, OAS2, OAS3, STAT1, CXCL10, and IFITM3 (**Figure 4A, E**). **Figure 4F** shows the expression of various genes encoding SIGLEC proteins that are responsible for regulating microglial cell□cell interactions [Reviewed in (Crocker, Paulson, and Varki 2007)]. Consistent with previous studies, we found that HIV-1 infection causes significant upregulation of SIGLEC1, which has been implicated in the direct cell□cell transmission of HIV (Izquierdo-Useros et al. 2012; Zou et al. 2011). However, we found that SIGLEC11 and SIGLEC16 were significantly downregulated after infection.

We then validated the expression of a subset of the ISGs identified in the sequencing dataset by RT-qPCR of JRFL infected 03SF iPSC-derived microglia. We found significant upregulation of CXCL10, RSAD2, ISG15, and IDO1 (**Figure 4G**). Elevated expression of these genes persisted over an additional week of infection on day 23 (**Figure 4G**). Additionally, we performed RT-qPCR on CD06 iPSC-derived microglia infected with either JRFL or YU2 HIV strains. We also found increased expression of CXCL10 and RSAD2 in these HIV-infected cells; however, only the day 16 YU2 condition reached significance (**Figure 4H**). Comparison of Figure 4G and 4H indicates potential differences with infecting different cell lines. Together, these data support the conclusion that HIV-1 infection induces sustained type I interferon signaling in iPSC-derived microglia and alters the gene regulation of many microglial biological processes including interferon signaling.

HIV-1 infected microglia incorporate into cerebral organoids

After characterizing the response of isolated human iPSC-derived microglia to HIV-1 infection we then investigated whether HIV-1 infected microglia could incorporate into iPSC-derived cerebral organoids and whether interferon signaling was similarly upregulated in microglia and potentially other neural cell types. Cerebral organoids were grown using modified, published protocols (Lancaster and Knoblich 2014; Paşca et al. 2015; Sloan et al. 2018; Yoon et al. 2019; Qian et al. 2020; Xu et al. 2021). To create microglia-containing organoids, we cocultured human microglia with sliced neocortical organoids (SNO), prepared as described previously (Qian et al. 2020). SNOs exhibit enhanced neurogenesis and laminar expansion (Qian et al. 2020). We found that microglia exhibit the ability to incorporate with organoid slices to form human microglia containing sliced neocortical organoids (mSNOs). **Figure 5A** shows mSNO containing neurons ($MAP2^+$), astrocytes ($GFAP^+$), and microglia ($IBA1^+$). These neuroimmune organoids provide a model system for studying the impact of HIV-1 infection on the physiology, localization, and interactions of these three cell types.

To create an HIV-1 infected human cerebral organoid, we infected 03SF iPSC-derived microglia with JRFL HIV. Following 2 weeks in culture, infected or noninfected microglia were added to 400 µM organoid slices and cultured for 2 additional weeks. On day 14 post coculture with microglia, mSNOs were fixed for immunohistochemistry or total RNA was extracted for RT-qPCR analysis. HIV-1-infected microglia ($p24^+$, $IBA1^+$) were detected in a mSNO (**Figure 5B&C**). Interestingly, neurons ($MAP2^+$) appeared to be sparser in regions of HIV-1-infected microglia (**Figure 5B** "arrows"). These regions had scattered $MAP2^+$ processes (**Figure 5B1**) compared with the denser MAP2 staining throughout the bulk of the organoid. HIV-1 *gag/pol* RNA exhibited significant expression in mSNOs containing HIV-1 infected microglia (**Figure 5D**). To provide evidence of productive infection in mSNOs, we identified secreted p24 only in the media of organoid cultures that had received HIV-1 infected microglia (**Figure 5E**).

Because we observed significant and sustained interferon signaling in microglial monocultures, we evaluated mRNA expression of a panel of ISGs (ISG15, RSAD2, IFITM3,

MX1, IFI44, IFI27). We found that ISG15 mRNA was significantly upregulated and RSAD2 also showed an increasing trend of expression in mSNOs containing HIV-1 infected microglia (**Figure 5F**). IFITM3 has been touted as a marker for interferon-responsive microglia and has been shown to play a newly discovered role in amyloid precursor protein processing to amyloid beta (Hur et al. 2020). Interestingly, we found significant upregulation of IFITM3 mRNA in mSNOs containing HIV-1 infected microglia (**Figure 5F).** We also evaluated the expression of MX1, IFI27, and IFI44, which, along with ISG15 and RSAD2, were among the top 10 persistently upregulated genes in a recent study on two cohorts of 22 HIV-1 seroconverts from Uganda and 22 from South Africa (Mackelprang et al. 2023). Expression of MX1, IFI27, and IFI44 appeared to be increased but failed to reach significance. Especially considering the small fraction of HIV-1 infected microglia in the cultured mSNO (**Figure 5B**), these increases suggest that HIV-1 infected microglia are associated with increased interferon signaling in the organoids and may have indirect consequences for neuronal viability and inflammatory responses in other cell types.

DISCUSSION:

In this study, we used iPSC-derived human microglia and microglia containing cortical organoids to model HIV-1 related neuroimmune dysregulation and pathology. In this model, iPSC-derived microglia were shown to be infected with two strains of replication competent HIV-1, JRFL and YU2, and exhibited inflammatory activation, as shown by gene expression changes and cytokine/chemokine secretion (**Figures 2 & 3**). Importantly, we found persistent activation of type I interferon response pathways and downstream interferon stimulated genes (ISGs), which may have important implications for understanding the pathogenesis of HAND.

In comparison to the recently developed primary human neural progenitor cell-derived organoid HIV-1 model (dos Reis et al. 2020) and the 2D neuron, astrocyte, and microglia "triculture" HIV-1 model (Ryan et al. 2020), an iPSC-derived human microglia containing sliced

neocortical organoid model has distinct advantages. Organoids recapitulate 3D cell-cell and cell-matrix interactions more faithfully than 2D cultures and develop complex tissue architecture (Lancaster et al. 2013; Paşca et al. 2015; Birey et al. 2017; Quadrato et al. 2017; Velasco et al. 2019); thus, organoids are well suited to studying aspects of altered brain anatomy and physiology seen in individuals with *HAND* (Di Sclafani et al. 1997; Clifford et al. 2017; Israel et al. 2019). While others have also generated microglia containing organoids using a protocol in which microglia innately develop within organoids, this system is associated with a high degree of heterogeneous cell types (Gumbs et al. 2022), which could make dissection of the relative contributions and effects on specific cell types more complex. In our method, we have greater freedom to manipulate the timing, proportion, and infection stage of microglia addition in sliced neocortical organoids. While some previous studies used pseudotyped virus (dos Reis et al. 2020), our study examined infection using two macrophage tropic, replication competent strains of HIV-1. Our findings, showing induction of inflammatory gene expression associated with active viral expression align with recent studies on brain samples from HIV-1^{+} patients from the National NeuroAIDS Tissue Consortium (NNTC). In that study, HIV-1 RNA load was found to correlate with increased interferon signaling and inflammatory gene sets while inversely correlating with neuronal and synaptic gene sets, suggesting neuronal pathology (Sanna et al. 2021).

Microglia secrete diverse cytokines and chemokines implicated in HIV-1 neuropathology (Hanisch 2002; Ramesh, MacLean, and Philipp 2013; Chen et al. 2017). Cytokine/chemokine analysis of the supernatant of HIV-1 infected microglia identified the secretion of M-CSF and IP-10/CXCL10 (**Figure 2F**). M-CSF overexpression has been linked to microglial proliferation, increased phagocytosis, cytokine secretion, and inflammatory responses in both Alzheimer's disease (AD) and HAND, as well as increased microglial susceptibility to HIV-1 infection and increased virus replication (Gallo et al. 1990; Kalter et al. 1991; Kutza et al. 2000; Mitrasinovic et al. 2001; Kutza, Fields, Grimm, and Clouse 2002; Smith et al. 2013). IP-10/CXCL10 is a

chemotactic chemokine that recruits leukocytes, T cells, and monocytes while also being neurotoxic and strongly correlated with HIV-1 related disease progression (van Marle et al. 2004; Jiao et al. 2012; Lei, Yin, Shang, and Jiang 2019). Clinical studies have shown elevated IP-10/CXCL10 levels (~200-1000 pg/ml) in the cerebral spinal fluid of HIV-1^{+} individuals (Kolb et al. 1999; Peluso et al. 2017); these levels are strikingly similar to our observations (**Figure 2F**). CXCL10/IP-10 has been shown to be induced by HIV-1 proteins gp120, Nef, and Tat (Kutsch, Oh, Nath, and Benveniste 2000; Asensio et al. 2001; van Marle et al. 2004; Lei, Yin, Shang, and Jiang 2019). Importantly, IP-10/CXCL10 and RANTES (CCL5) were the strongest predictors of neurocognitive impairment in a screen of 139 HIV-1^{+} individuals (Ruhanya et al. 2021), similar to findings from earlier studies (Valverde-Villegas et al. 2018; Burlacu et al. 2020). HIV-1 brain infection leads to an abnormal inflammatory state and dysregulated cytokine/chemokine production (Kaul, Garden, and Lipton 2001; González-Scarano and Martín-García 2005; Burdo, Lackner, and Williams 2013). Despite this knowledge, there remains a large gap in our understanding of how CXCL10 and other cytokines/chemokines associated with CNS HIV-1 infection alter aspects of neuronal excitability, synaptic transmission, and inward and outward currents vital to healthy neuronal physiology.

A striking finding in our study was the persistent activation of interferon response genes. Induction of these pathways is known to be a hallmark of HIV-1 infection in monocytes and macrophages, much more prominently than in T cells (Berg et al. 2014; Aso, Ito, Koyanagi, and Sato 2019; Elsner et al. 2020; Jeremiah et al. 2023). Thus, it is not surprising to have seen this strong response in microglia, which share many physiologic properties with macrophages [reviewed in (Li and Barres 2018)]. Most studies suggest that the interferon response is relatively transient; thus, the persistent expression of at least a subset of ISGs may be a relatively unique feature of microglial HIV-1 infection that may have important pathophysiologic consequences. Increasing evidence suggests a role for type I interferons in cognitive-related deficits seen in patients with various neurodegenerative diseases. Using single-cell sequencing,

researchers have dissected a unique sub-population of interferon-responsive microglia that may potentiate dysregulated immune interactions in the form of aberrant pruning of synapses, altered phagocytic function, and dysregulated cytokine/chemokine production (Jin et al. 2022). Constitutive overexpression of type I interferons seen in the “interferonopathies” can be associated with profound CNS disease [reviewed in (Goldmann, Blank, and Prinz 2016), and (Blank and Prinz 2017)](Wiley, Steinman, and Wang 2023). Patients receiving type I interferons therapeutically may experience cognitive impairment and neurological symptoms (Christina, Randall, and Arthur 1991; Pavol et al. 1995; Capuron, Ravaud, and Dantzer 2001; Capuron et al. 2002; Wichers et al. 2005; Raison, Demetrashvili, Capuron, and Miller 2005).

Whether interferon induction inhibits or enhances HIV infection and latency in microglia remains to be understood. Recent studies have highlighted that interferon can inhibit HIV infection of primary microglia but less so of iPSC-derived microglia, as well as macrophages (Nasr et al. 2017; Woodburn et al. 2022). Interestingly, interferon may promote latency in macrophages (Dickey, Martins, Planelles, and Hanley 2022). An important feature of HIV infection of microglia identified in previous in vitro studies has been the rapid induction of viral latency (Alvarez-Carbonell et al. 2019; Sreeram et al. 2022). Our cerebral organoid model will provide an interesting system to examine the induction of HIV latency, its reactivation, and its effects on both adjacent and more distant neural cells.

An important future direction, facilitated by the development of this model system, will be experiments aimed at understanding the functional consequences that HIV infection, dysregulated interferon signaling, inflammatory activity, and changes in other important genes expressed in the CNS, may have on neuronal synaptic transmission. A number of ISGs have predicted downstream effects that could trigger or enhance neurodegeneration. For example, indoleamine 2,3-dioxygenase 1 (IDO) is a key enzyme in tryptophan catabolism, leading to the formation of kynurenic acid, an antagonist of NMDA receptors (Schwarcz and Stone 2017). This pathway and its products, such as the neurotoxin and NMDAR antagonist quinolinic acid, have

been previously implicated in neurodegenerative diseases, including Huntington's, Alzheimer's and Parkinson's disease (Malpass 2011; Maddison and Giorgini 2015).

Overall, the HIV-1 mSNO model presents an effective in vitro platform for investigating the underlying molecular and cellular mechanisms associated with HIV-1 and human neural cell interactions. **Our results predict that interferon stimulated genes likely play a role in altering neuronal function and contributing to HAND.**

ACKNOWLEDGEMENTS

This work was supported in part by grants from the NIH (R21NS120806), a Rutgers Busch Biomedical Grant, a Rutgers Brain Health Institute Pilot Grant, and the Robert Wood Johnson Foundation (Grant #74260). AJB was supported by NIH NIGMS T32GM8339 and NIH NCATS TL1TR003019.

AUTHOR CONTRIBUTIONS

AJB, ZPP, PJ, RPH, and ABR conceived the study. AJB designed the experiments and interpreted the data. AJB performed most of the experiments with technical assistance from ACS, HL, and YA. ACS and AJB performed qPCR. HL and AJB performed ELISA. AJB performed immunocytochemistry, immunohistochemistry, and confocal imaging. AJB and HS performed viral infections. RPH and AJB performed computational analysis of RNA-seq data. AJB prepared the figures and wrote the manuscript with input from all coauthors.

COMPETING FINANCIAL INTERESTS

The authors declare no competing financial interests.

METHODS

Human induced pluripotent stem cell maintenance

Three human iPSC lines were used in this study (male 03SF iPSC line; female CD06 iPSC line; male CD52 iPSC line). Human iPSCs were cultured in stem cell medium consisting of MACs iPS-Brew XF complete media. The culture medium was changed daily. Human iPSCs were passaged one to two times per week onto new plates coated with Matrigel. Human iPSCs were detached with Accutase treatment for 5 min and centrifuged at 120 rcf for 5 min. The pellet was resuspended in stem cell medium plus Y-27632 (10 µM). The iPSCs used in this study were below passage 50. All studies were performed with protocols approved by Rutgers University.

Generation of microglia

Primitive microglia precursors (PMPs) were generated from 3 iPSC cell lines using a previously established protocol (Haenseler et al. 2017). iPSCs were detached with Accutase, plated at 20,000 cells per well in a 96-well low-adherence plate in yolk sac induction medium plus the rock inhibitor Y-27632 (10 µM), and centrifuged at 1000 rpm for 3 min to aggregate the cells for embryoid body formation. Yolk-sac induction medium consisted of MAC iPS-Brew XF complete media plus bone morphogenetic protein 4 (BMP4, 50 ng/ml), vascular endothelial growth factor (VEGF, 50 ng/ml), stem cell factor (SCF, 20 ng/ml), and ß-mercaptoethanol. Yolk-sac induction media was given for the first 5 days of culture. On day 6, YS-EBs were plated in 100 mm cell culture plates in factory media consisting of XVIVO15 supplemented with 0.5% NEAA, ß-mercaptoethanol, macrophage colony stimulating factor (M-CSF, 100 ng/ml) and interleukin-3 (25 ng/ml). At 2-4 weeks after plating, human PMPs egress from the yolk sac lumen into the surrounding media and are continuously produced for more than 3 months.

To mature PMPs into microglia, PMPs were transitioned to maturation media composed of XVIVO15 supplemented with N2, Glutamax, 0.5% NEAA, interleukin-34 (IL-34, 100 ng/ml),

granulocyte macrophage colony stimulating factor (GM-CSF, 10 ng/ml, and M-CSF (25 ng/ml) for 1-2 weeks. The medium was changed every 4 days. Cells were then detached with 20 min Accutase treatment and used for experiments.

Generation of iPSC-derived Cerebral Organoids

Cerebral organoids were generated from 1 iPSC line using adapted previously published protocols (Qian et al. 2020). In this study, 9,000 iPSCs were cultured in low-adherence 96-well plates to form uniform embryoid bodies. On day 1, the medium was changed to neural induction medium composed of DMEM/F12 supplemented with 1X N2, 2 µM A83-01, and 2 µM dorsomorphin. On days 5 and 6, half of the medium was replaced with DMEM/F12 supplemented with 1X N2, 10 µM SB431542, and 1 µM CHIR99021. On day 7, EBs were embedded in a Growth-Factor-Reduced Matrigel 'cookie' as previously described (Qian et al. 2020). Half of the medium was changed every two days until day 14. On day 14, organoids were dissociated from the Matrigel cookie and placed in low-adherence 6-well plates on an orbital shaker at 85 rpm. On day 16, organoids were fed 1:1 DMEF12: Neurobasal, 1X N2, 1X B27-RA, 0.5% NEAA, and 200 µM L-AA. Media was replenished every 2-3 days until day 30. On day 30, the medium was changed to 1:1 DMEF12: Neurobasal, 1X N2, 1X B27, 0.5% NEAA, 200 µM L-AA, and.25% GFR-Matrigel. Half of the media was changed every 3-4 days.

Organoid Slicing

To create sliced neocortical organoid cultures, cerebral organoids were sectioned with a vibratome and transferred back into in vitro cell culture. Briefly, a fresh stock of 3% low-melting temperature agarose in PBS was prepared and kept at 39°C to remain liquid. Artificial cerebral spinal fluid (ACSF) for sectioning contained (in mM): NaCl 125, KCl 2.5, $NaH_2PO_4 \cdot H_2O$ 1.25, $NaHCO_3$ 25, $MgCl_2$ 1.2, $CaCl_2$ 2.5, glucose ($C_6H_{12}O_6$) 2.5, and sucrose ($C_{12}H_{22}O_{11}$) 22.5. The ACSF was then bubbled with 5% CO_2/95% O_2 for 10 minutes before bivalent cations (in mM):

$MgCl_2$ 1.2, $CaCl_2$ 0.625. The solution was then filtered through a 0.2-micron PES filter and returned to bubbling on ice. Cerebral organoids were then transferred to 37°C DMEF12, 200 µM L-AA, and 55 µM beta-mercaptoethanol before being embedded in 3% low-melting temperature agarose. The agarose block containing organoids was then sectioned at 400 µM thickness. Slices were then subjected to two washing processes in Primocin-treated media to reduce the chance of contamination.

HIV-1 Stock Preparation

HIV-1 JRFL virus (ARP-395) and HIV-1 YU2 proviral DNA (ARP-1350) were obtained through the NIH HIV Reagent Program, Division of AIDS, NIAID. HIV-1 JRFL was propagated in phytohemagglutinin (PHA, 5 µg/ml)-stimulated human peripheral blood mononuclear cells. Viruses were harvested on days 7-10 post infection. HIV-1 YU2 stocks were generated by transfection of 293T cells with HIV-1 YU2 proviral DNA. The transfected cells were cocultivated with PHA-PBMCs 48 h after transfection, and cell supernatants were harvested 7 days after coculture. The YU2 HIV stocks were further propagated in PHA-PBMCs as described. The amount of viral p24 was determined using the HIV-1 Gag p24 DuoSet ELISA (R &D System, DY7360-05).

HIV-1 infection

PMPs were matured for 1-2 weeks in microglia maturation medium. Matured PMPs were then incubated with 2 ng/ml p24 of either JRFL strain or YU2 strain HIV-1 (NIH AIDS Repository) for 24 hours at 300,000 cells per 100 µl of media. After 24 hours, DMEF12 was added, and the cells were centrifuged for 3 min at 120 rcf. The cells were then resuspended in microglia maturation media minus M-CSF and plated. Half of the media was changed every 3-6 days.

HIV-1 2-LTR circles PCR

For detection of HIV 2LTR circles, total DNA (including small nongenomic DNA) was isolated with a DNeasy Blood and Tissue kit (Qiagen 69504). End point PCR analysis (Taq 2X Master Mix, NEB) was performed using 300 ng DNA template and 2-LTR circle primers: forward, MH535: 5′-AACTAGGGAACCCACTGCTTAAG-3′; reverse, MH536: 5′-TCCACAGATCAAGGATATCTTGTC-3′ (Butler, Hansen, and Bushman 2001).

Tissue preparation

Organoids were fixed in 4% PFA overnight at 4°C. Organoids were then transferred to 15% sucrose and 0.05% sodium azide in PBS for 24 hours, followed by another 24 hours in 30% sucrose and 0.05% sodium azide in PBS. Organoids were then embedded in OCT freezing medium and snap frozen on an ethanol dry ice slurry. Frozen embedded organoids were given at least 3 hours to warm to -20°C before cryosectioning on a Leica cryostat at thicknesses between 10-30 µM. Sections were mounted on charged microscope slides (VWR) and placed on a slide warmer at 37°C for 30 min. Slides were then stored in a slide box at -20°C until used for staining.

Immunofluorescence

For immunocytochemistry, half of the medium was left in each well with an equal amount of 4% PFA and then added at a final concentration of 2% PFA overnight at 4°C. The next day, PFA was removed, and the cells were washed with PBS plus 0.3 M glycine for 30 min. The cells were then permeabilized with 0.2% Triton X-100 in PBS for 7 min. The cells were then blocked for 1 hour in blocking buffer consisting of 5% normal goat serum (NGS), 4% bovine serum albumin (BSA), 0.05% Triton X-100, 0.05% sodium azide, and PBS.

For immunohistochemistry, cryosectioned organoid slides were warmed to 37°C for 5 min. A hydrophobic barrier was then drawn around the specimens and allowed to dry for 5 min. PBS plus 0.3 M glycine was then added in a liquid dome over the specimens to rehydrate for 10

min. Sections were permeabilized with 0.5% Triton X-100, 0.3 M glycine, and PBS for 1 hr. After permeabilization, the sections were blocked with blocking solution consisting of 5% normal goat serum, 4% BSA, 0.05% Triton X-100, 0.05% sodium azide, and PBS for 1 hr. Primary antibodies were diluted in blocking solution and applied to the sections overnight at 4°C. The primary antibodies and their dilutions are summarized in the Key Resources Table. After washing with 0.05% Triton X-100 and PBS (PBST) 5 times, secondary antibodies diluted in blocking buffer were added for 1 hr at RT. Finally, the sections were washed five times with PBST before a final wash in deionized water and mounting with DAPI Fluoroshield (Fisher). Secondary antibodies were Alexa Fluor 488-, 546-, 633- or 647-conjugated goat antibodies (Invitrogen) used at a 1:500 dilution. Images were taken on a Zeiss LSM700 confocal microscope.

RNA isolation

Total RNA was prepared with an RNeasy Plus kit (Qiagen) with preprocessing through Qiashredder (Qiagen) and frozen at -80°C.

RT-qPCR

cDNA was generated using SuperScript VILO Master mix. RNA expression was measured using SYBR green on a QuantStudio 3 (Agilent). Probes were generated using NCBI primer blast and are listed in Table X. Two technical replicates were performed per sample. When a high standard deviation between replicates occurred, replicates were rerun in triplicate. All expression levels were normalized to GAPDH expression and represented as $2^{-(\Delta\Delta CT)}$. For null result values where a ct was not achieved, a max ct value of 40 was used for statistical analysis.

Bulk RNA sequencing and analysis

We performed bulk RNA-sequencing analysis of iPSC-derived microglia. Total RNA was prepared using an RNeasy kit (QIAGEN). Library construction and sequencing were performed by Novogene. The libraries were subjected to 75 bp paired read sequencing using a NextSeq500 Illumina sequencer. Approximately 30–36 million paired reads were generated for each sample. Bc12Fastq software, version 1.8.4, was used to generate Fastq files. The genome sequence was then indexed using the rsem-prepare-reference command.

Each fastq file was trimmed and checked for quality with fastp (v. 0.12.2) and then aligned to the UCSC hg38 human genome using HISAT2 (v.2.1.0)71,72. Transcript counts were extracted using the featureCounts function of the Rsubread package.

Statistics and reproducibility. All data represent the mean ± s.e.m. When only two independent groups were compared, significance was determined by a two-tailed unpaired t test with Welch's correction. A p value <0.05 was considered significant. The analyses were performed in GraphPad Prism v.9. All experiments were independently performed at least three times with similar results.

References:

Abud, Edsel M., Ricardo N. Ramirez, Eric S. Martinez, Luke M. Healy, Cecilia H. H. Nguyen, Sean A. Newman, Andriy V. Yeromin, Vanessa M. Scarfone, Samuel E. Marsh, Cristhian Fimbres, Chad A. Caraway, Gianna M. Fote, Abdullah M. Madany, Anshu Agrawal, Rakez Kayed, Karen H. Gylys, Michael D. Cahalan, Brian J. Cummings, Jack P. Antel, Ali Mortazavi, Monica J. Carson, Wayne W. Poon, and Mathew Blurton-Jones. 2017. 'iPSC-Derived Human Microglia-like Cells to Study Neurological Diseases', *Neuron*, 94: 278-93.e9.

Alvarez-Carbonell, D., F. Ye, N. Ramanath, Y. Garcia-Mesa, P. E. Knapp, K. F. Hauser, and J. Karn. 2019. 'Cross-talk between microglia and neurons regulates HIV latency', *PLoS Pathog*, 15: e1008249.

Alvarez-Carbonell, David, Fengchun Ye, Nirmala Ramanath, Yoelvis Garcia-Mesa, Pamela E. Knapp, Kurt F. Hauser, and Jonathan Karn. 2020. 'Cross-talk between microglia and neurons regulates HIV latency', *PLOS Pathogens*, 15: e1008249.

Anderson, Albert M., Jeffrey L. Lennox, Mark M. Mulligan, David W. Loring, Henrik Zetterberg, Kaj Blennow, Cari Kessing, Rajeth Koneru, Kirk Easley, and William R. Tyor. 2017. 'Cerebrospinal fluid interferon alpha levels correlate with neurocognitive impairment in ambulatory HIV-Infected individuals', *Journal of NeuroVirology*, 23: 106-12.

Asensio, V. C., J. Maier, R. Milner, K. Boztug, C. Kincaid, M. Moulard, C. Phillipson, K. Lindsley, T. Krucker, H. S. Fox, and I. L. Campbell. 2001. 'Interferon-independent, human immunodeficiency virus type 1 gp120-mediated induction of CXCL10/IP-10 gene expression by astrocytes in vivo and in vitro', *Journal of Virology*, 75: 7067-77.

Aso, H., J. Ito, Y. Koyanagi, and K. Sato. 2019. 'Comparative Description of the Expression Profile of Interferon-Stimulated Genes in Multiple Cell Lineages Targeted by HIV-1 Infection', *Front Microbiol*, 10: 429.

Baruch, Kuti, Aleksandra Deczkowska, Eyal David, Joseph M. Castellano, Omer Miller, Alexander Kertser, Tamara Berkutzki, Zohar Barnett-Itzhaki, Dana Bezalel, Tony Wyss-Coray, Ido Amit, and Michal Schwartz. 2014. 'Aging-induced type I interferon response at the choroid plexus negatively affects brain function', *Science*, 346: 89-93.

Berg, R. K., S. H. Rahbek, E. Kofod-Olsen, C. K. Holm, J. Melchjorsen, D. G. Jensen, A. L. Hansen, L. B. Jørgensen, L. Ostergaard, M. Tolstrup, C. S. Larsen, S. R. Paludan, M. R. Jakobsen, and T. H. Mogensen. 2014. 'T cells detect intracellular DNA but fail to induce type I IFN responses: implications for restriction of HIV replication', *PLoS One*, 9: e84513.

Birey, Fikri, Jimena Andersen, Christopher D. Makinson, Saiful Islam, Wu Wei, Nina Huber, H. Christina Fan, Kimberly R. Cordes Metzler, Georgia Panagiotakos, Nicholas Thom, Nancy A. O'Rourke, Lars M. Steinmetz, Jonathan A. Bernstein, Joachim Hallmayer, John R. Huguenard, and Sergiu P. Paşca. 2017. 'Assembly of functionally integrated human forebrain spheroids', *Nature*, 545: 54-59.

Blank, T., and M. Prinz. 2017. 'Type I interferon pathway in CNS homeostasis and neurological disorders', *Glia*, 65: 1397-406.

Burdo, Tricia H., Andrew Lackner, and Kenneth C. Williams. 2013. 'Monocyte/macrophages and their role in HIV neuropathogenesis', *Immunological Reviews*, 254: 102-13.

Burlacu, R., A. Umlauf, T. D. Marcotte, B. Soontornniyomkij, C. C. Diaconu, A. Bulacu-Talnariu, A. Temereanca, S. M. Ruta, S. Letendre, L. Ene, and C. L. Achim. 2020. 'Plasma CXCL10 correlates with HAND in HIV-infected women', *Journal of NeuroVirology*, 26: 23-31.

44 Butler, S. L., M. S. Hansen, and F. D. Bushman. 2001. 'A quantitative assay for HIV DNA integration in
45 vivo', *Nat Med*, 7: 631-4.
46 Byrnes, S. J., T. A. Angelovich, K. Busman-Sahay, C. R. Cochrane, M. Roche, J. D. Estes, and M. J.
47 Churchill. 2022. 'Non-Human Primate Models of HIV Brain Infection and Cognitive Disorders',
48 *Viruses*, 14.
49 Capuron, Lucile, Jane F. Gumnick, Dominique L. Musselman, David H. Lawson, Andrea Reemsnyder,
50 Charles B. Nemeroff, and Andrew H. Miller. 2002. 'Neurobehavioral Effects of Interferon-α in
51 Cancer Patients: Phenomenology and Paroxetine Responsiveness of Symptom Dimensions',
52 *Neuropsychopharmacology*, 26: 643-52.
53 Capuron, Lucile, Alain Ravaud, and Robert Dantzer. 2001. 'Timing and Specificity of the Cognitive
54 Changes Induced by Interleukin-2 and Interferon-α Treatments in Cancer Patients',
55 *Psychosomatic Medicine*, 63.
56 Casano, Alessandra Maria, and Francesca Peri. 2015. 'Microglia: Multitasking Specialists of the Brain',
57 *Developmental Cell*, 32: 469-77.
58 Chargelegue, Daniel, and Carol M. O'Toole. 1992. 'Development of a sensitive ELISA for HIV-1 p24
59 antigen using a fluorogenic substrate for monitoring HIV-1 replication in vitro', *Journal of*
60 *Virological Methods*, 38: 323-32.
61 Chen, Natalie C., Andrea T. Partridge, Christian Sell, Claudio Torres, and Julio Martín-García. 2017. 'Fate
62 of microglia during HIV-1 infection: From activation to senescence?', *Glia*, 65: 431-46.
63 Christina, A. Meyers, S. Scheibel Randall, and D. Forman Arthur. 1991. 'Persistent neurotoxicity of
64 systemically administered interferon-alpha', *Neurology*, 41: 672.
65 Claes, Christel, Johanna Van den Daele, and Catherine M. Verfaillie. 2018. 'Generating tissue-resident
66 macrophages from pluripotent stem cells: Lessons learned from microglia', *Cellular*
67 *Immunology*, 330: 60-67.
68 Clifford, Katherine M., Vishal Samboju, Yann Cobigo, Benedetta Milanini, Gabriel A. Marx, Joanna M.
69 Hellmuth, Howard J. Rosen, Joel H. Kramer, Isabel E. Allen, and Victor G. Valcour. 2017.
70 'Progressive Brain Atrophy Despite Persistent Viral Suppression in HIV Patients Older Than 60
71 Years', *Journal of acquired immune deficiency syndromes (1999)*, 76: 289-97.
72 Crocker, Paul R., James C. Paulson, and Ajit Varki. 2007. 'Siglecs and their roles in the immune system',
73 *Nature Reviews Immunology*, 7: 255-66.
74 Di Sclafani, V., R. D. Mackay, D. J. Meyerhoff, D. Norman, M. W. Weiner, and G. Fein. 1997. 'Brain
75 atrophy in HIV infection is more strongly associated with CDC clinical stage than with cognitive
76 impairment', *Journal of the International Neuropsychological Society : JINS*, 3: 276-87.
77 Dickey, L. L., L. J. Martins, V. Planelles, and T. M. Hanley. 2022. 'HIV-1-induced type I IFNs promote viral
78 latency in macrophages', *J Leukoc Biol*, 112: 1343-56.
79 Dos Reis, R. S., S. Sant, and V. Ayyavoo. 2023. 'Three-Dimensional Human Brain Organoids to Model
80 HIV-1 Neuropathogenesis', *Methods Mol Biol*, 2610: 167-78.
81 dos Reis, Roberta S., Shilpa Sant, Hannah Keeney, Marc C. E. Wagner, and Velpandi Ayyavoo. 2020.
82 'Modeling HIV-1 neuropathogenesis using three-dimensional human brain organoids (hBORGs)
83 with HIV-1 infected microglia', *Scientific Reports*, 10: 15209.
84 Durafourt, B. A., C. S. Moore, D. A. Zammit, T. A. Johnson, F. Zaguia, M. C. Guiot, A. Bar-Or, and J. P.
85 Antel. 2012. 'Comparison of polarization properties of human adult microglia and blood-derived
86 macrophages', *Glia*, 60: 717-27.

87 Eggers, C., G. Arendt, K. Hahn, I. W. Husstedt, M. Maschke, E. Neuen-Jacob, M. Obermann, T.
88 Rosenkranz, E. Schielke, and E. Straube. 2017. 'HIV-1-associated neurocognitive disorder:
89 epidemiology, pathogenesis, diagnosis, and treatment', *J Neurol*, 264: 1715-27.
90 Elsner, C., A. Ponnurangam, J. Kazmierski, T. Zillinger, J. Jansen, D. Todt, K. Döhner, S. Xu, A. Ducroux,
91 N. Kriedemann, A. Malassa, P. K. Larsen, G. Hartmann, W. Barchet, E. Steinmann, U. Kalinke, B.
92 Sodeik, and C. Goffinet. 2020. 'Absence of cGAS-mediated type I IFN responses in HIV-1-
93 infected T cells', *Proc Natl Acad Sci U S A*, 117: 19475-86.
94 Eugenin, E. A., and J. W. Berman. 2016. 'Improved Methods to Detect Low Levels of HIV Using
95 Antibody-Based Technologies', *Methods Mol Biol*, 1354: 265-79.
96 Gallo, Paolo, Silvana Pagni, Bruno Giometto, Maria G. Piccinno, Felice Bozza, Vincenza Argentiero, and
97 Bruno Tavolato. 1990. 'Macrophage-colony stimulating factor (M-CSF) in the cerebrospinal
98 fluid', *Journal of Neuroimmunology*, 29: 105-12.
99 Gendelman, Howard E., Stuart A. Lipton, Marc Tardieu, Michael I. Bukrinsky, and Hans S. L. M. Nottet.
100 1994. 'The neuropathogenesis of HIV-1 infection', *Journal of Leukocyte Biology*, 56: 389-98.
101 Goldmann, T., T. Blank, and M. Prinz. 2016. 'Fine-tuning of type I IFN-signaling in microglia--
102 implications for homeostasis, CNS autoimmunity and interferonopathies', *Curr Opin Neurobiol*,
103 36: 38-42.
104 González-Scarano, Francisco, and Julio Martín-García. 2005. 'The neuropathogenesis of AIDS', *Nature*
105 *Reviews Immunology*, 5: 69-81.
106 Gosselin, David, Dylan Skola, Nicole G. Coufal, Inge R. Holtman, Johannes C. M. Schlachetzki, Eniko
107 Sajti, Baptiste N. Jaeger, Carolyn O'Connor, Conor Fitzpatrick, Martina P. Pasillas, Monique
108 Pena, Amy Adair, David D. Gonda, Michael L. Levy, Richard M. Ransohoff, Fred H. Gage, and
109 Christopher K. Glass. 2017. 'An environment-dependent transcriptional network specifies
110 human microglia identity', *Science*, 356: eaal3222.
111 Gumbs, Stephanie B. H., Amber Berdenis van Berlekom, Raphael Kübler, Pauline J. Schipper, Lavina
112 Gharu, Marco P. Boks, Paul R. Ormel, Annemarie M. J. Wensing, Lot D. de Witte, and Monique
113 Nijhuis. 2022. "Characterization of HIV-1 Infection in Microglia-Containing Human Cerebral
114 Organoids." In *Viruses*.
115 Haenseler, W., S. N. Sansom, J. Buchrieser, S. E. Newey, C. S. Moore, F. J. Nicholls, S. Chintawar, C.
116 Schnell, J. P. Antel, N. D. Allen, M. Z. Cader, R. Wade-Martins, W. S. James, and S. A. Cowley.
117 2017. 'A Highly Efficient Human Pluripotent Stem Cell Microglia Model Displays a Neuronal-Co-
118 culture-Specific Expression Profile and Inflammatory Response', *Stem Cell Reports*, 8: 1727-42.
119 Hammond, Timothy R., Connor Dufort, Lasse Dissing-Olesen, Stefanie Giera, Adam Young, Alec
120 Wysoker, Alec J. Walker, Frederick Gergits, Michael Segel, James Nemesh, Samuel E. Marsh,
121 Arpiar Saunders, Evan Macosko, Florent Ginhoux, Jinmiao Chen, Robin J. M. Franklin, Xianhua
122 Piao, Steven A. McCarroll, and Beth Stevens. 2019. 'Single-Cell RNA Sequencing of Microglia
123 throughout the Mouse Lifespan and in the Injured Brain Reveals Complex Cell-State Changes',
124 *Immunity*, 50: 253-71.e6.
125 Hanisch, U. K. 2002. 'Microglia as a source and target of cytokines', *Glia*, 40: 140-55.
126 Hofer, Markus J., and Iain L. Campbell. 2013. 'Type I interferon in neurological disease—The devil from
127 within', *Cytokine & Growth Factor Reviews*, 24: 257-67.
128 Hur, J. Y., G. R. Frost, X. Wu, C. Crump, S. J. Pan, E. Wong, M. Barros, T. Li, P. Nie, Y. Zhai, J. C. Wang, J.
129 Tcw, L. Guo, A. McKenzie, C. Ming, X. Zhou, M. Wang, Y. Sagi, A. E. Renton, B. T. Esposito, Y.
130 Kim, K. R. Sadleir, I. Trinh, R. A. Rissman, R. Vassar, B. Zhang, D. S. Johnson, E. Masliah, P.

131 Greengard, A. Goate, and Y. M. Li. 2020. 'The innate immunity protein IFITM3 modulates γ-
132 secretase in Alzheimer's disease', *Nature*, 586: 735-40.
133 Israel, Sarah M., Shiva Hassanzadeh-Behbahani, Peter E. Turkeltaub, David J. Moore, Ronald J. Ellis, and
134 Xiong Jiang. 2019. 'Different roles of frontal versus striatal atrophy in HIV-associated
135 neurocognitive disorders', *Human Brain Mapping*, 40: 3010-26.
136 Izquierdo-Useros, Nuria, Maier Lorizate, Maria C. Puertas, Maria T. Rodriguez-Plata, Nadine Zangger,
137 Elina Erikson, Maria Pino, Itziar Erkizia, Bärbel Glass, Bonaventura Clotet, Oliver T. Keppler,
138 Amalio Telenti, Hans-Georg Kräusslich, and Javier Martinez-Picado. 2012. 'Siglec-1 Is a Novel
139 Dendritic Cell Receptor That Mediates HIV-1 Trans-Infection Through Recognition of Viral
140 Membrane Gangliosides', *PLOS Biology*, 10: e1001448.
141 Jeremiah, N., H. Ferran, K. Antoniadou, K. De Azevedo, J. Nikolic, M. Maurin, P. Benaroch, and N.
142 Manel. 2023. 'RELA tunes innate-like interferon I/III responses in human T cells', *J Exp Med*, 220.
143 Jiao, Yanmei, Tong Zhang, Rui Wang, Hongwei Zhang, Xiaojie Huang, Jiming Yin, Liguo Zhang, Xiaoning
144 Xu, and Hao Wu. 2012. 'Plasma IP-10 Is Associated with Rapid Disease Progression in Early HIV-
145 1 Infection', *Viral Immunology*, 25: 333-37.
146 Jin, M., R. Xu, L. Wang, M. M. Alam, Z. Ma, S. Zhu, A. C. Martini, A. Jadali, M. Bernabucci, P. Xie, K. Y.
147 Kwan, Z. P. Pang, E. Head, Y. Liu, R. P. Hart, and P. Jiang. 2022. 'Type-I-interferon signaling drives
148 microglial dysfunction and senescence in human iPSC models of Down syndrome and
149 Alzheimer's disease', *Cell Stem Cell*, 29: 1135-53.e8.
150 Kalter, D. C., M. Nakamura, J. A. Turpin, L. M. Baca, D. L. Hoover, C. Dieffenbach, P. Ralph, H. E.
151 Gendelman, and M. S. Meltzer. 1991. 'Enhanced HIV replication in macrophage colony-
152 stimulating factor-treated monocytes', *J Immunol*, 146: 298-306.
153 Kaul, M., J. Zheng, S. Okamoto, H. E. Gendelman, and S. A. Lipton. 2005. 'HIV-1 infection and AIDS:
154 consequences for the central nervous system', *Cell Death Differ*, 12 Suppl 1: 878-92.
155 Kaul, Marcus, Gwenn A. Garden, and Stuart A. Lipton. 2001. 'Pathways to neuronal injury and
156 apoptosis in HIV-associated dementia', *Nature*, 410: 988-94.
157 Koenig, S., H. E. Gendelman, J. M. Orenstein, M. C. Dal Canto, G. H. Pezeshkpour, M. Yungbluth, F.
158 Janotta, A. Aksamit, M. A. Martin, and A. S. Fauci. 1986. 'Detection of AIDS virus in
159 macrophages in brain tissue from AIDS patients with encephalopathy', *Science*, 233: 1089-93.
160 Kolb, Stefan A., Bernd Sporer, Fritz Lahrtz, Uwe Koedel, Hans-Walter Pfister, and Adriano Fontana.
161 1999. 'Identification of a T cell chemotactic factor in the cerebrospinal fluid of HIV-1-infected
162 individuals as interferon-γ inducible protein 10', *Journal of Neuroimmunology*, 93: 172-81.
163 Koyanagi, Y., S. Miles, R. T. Mitsuyasu, J. E. Merrill, H. V. Vinters, and I. S. Chen. 1987. 'Dual infection of
164 the central nervous system by AIDS viruses with distinct cellular tropisms', *Science*, 236: 819-22.
165 Kraft-Terry, Stephanie D., Shilpa J. Buch, Howard S. Fox, and Howard E. Gendelman. 2009. 'A Coat of
166 Many Colors: Neuroimmune Crosstalk in Human Immunodeficiency Virus Infection', *Neuron*, 64:
167 133-45.
168 Krivine, A., G. Force, J. Servan, A. Cabée, F. Rozenberg, L. Dighiero, F. Marguet, and P. Lebon. 1999.
169 'Measuring HIV-1 RNA and interferon-alpha in the cerebrospinal fluid of AIDS patients: insights
170 into the pathogenesis of AIDS Dementia Complex', *J Neurovirol*, 5: 500-6.
171 Kutsch, O., J. Oh, A. Nath, and E. N. Benveniste. 2000. 'Induction of the chemokines interleukin-8 and
172 IP-10 by human immunodeficiency virus type 1 tat in astrocytes', *J Virol*, 74: 9214-21.

173 Kutza, J., K. Fields, T. A. Grimm, and K. A. Clouse. 2002. 'Inhibition of HIV replication and macrophage
174 colony-stimulating factor production in human macrophages by antiretroviral agents', *AIDS Res*
175 *Hum Retroviruses*, 18: 619-25.
176 Kutza, Joseph, Lynne Crim, Steven Feldman, Mark P. Hayes, Marion Gruber, Judy Beeler, and Kathleen
177 A. Clouse. 2000. 'Macrophage Colony-Stimulating Factor Antagonists Inhibit Replication of HIV-
178 1 in Human Macrophages', *The Journal of Immunology*, 164: 4955.
179 Lancaster, Madeline A., and Juergen A. Knoblich. 2014. 'Generation of cerebral organoids from human
180 pluripotent stem cells', *Nature Protocols*, 9: 2329-40.
181 Lancaster, Madeline A., Magdalena Renner, Carol-Anne Martin, Daniel Wenzel, Louise S. Bicknell,
182 Matthew E. Hurles, Tessa Homfray, Josef M. Penninger, Andrew P. Jackson, and Juergen A.
183 Knoblich. 2013. 'Cerebral organoids model human brain development and microcephaly',
184 *Nature*, 501: 373-79.
185 Lee, Jeong Seok, and Eui-Cheol Shin. 2020. 'The type I interferon response in COVID-19: implications for
186 treatment', *Nature Reviews Immunology*, 20: 585-86.
187 Lei, Jie, Xiaowan Yin, Hong Shang, and Yongjun Jiang. 2019. 'IP-10 is highly involved in HIV infection',
188 *Cytokine*, 115: 97-103.
189 Letendre, S. L., E. R. Lanier, and J. A. McCutchan. 1999. 'Cerebrospinal fluid beta chemokine
190 concentrations in neurocognitively impaired individuals infected with human immunodeficiency
191 virus type 1', *J Infect Dis*, 180: 310-9.
192 Lew, Brandon J., Timothy J. McDermott, Alex I. Wiesman, Jennifer Neill, Mackenzie S. Mills, Kevin R.
193 Robertson, Howard S. Fox, Susan Swindells, and Tony W. Wilson. 2018. 'Neural dynamics of
194 selective attention deficits in HIV-associated neurocognitive disorder', *Neurology*, 91: e1860.
195 Li, Qingyun, and Ben A. Barres. 2018. 'Microglia and macrophages in brain homeostasis and disease',
196 *Nature Reviews Immunology*, 18: 225-42.
197 Li, Y., J. C. Kappes, J. A. Conway, R. W. Price, G. M. Shaw, and B. H. Hahn. 1991. 'Molecular
198 characterization of human immunodeficiency virus type 1 cloned directly from uncultured
199 human brain tissue: identification of replication-competent and -defective viral genomes',
200 *Journal of Virology*, 65: 3973-85.
201 Lindl, Kathryn A., David R. Marks, Dennis L. Kolson, and Kelly L. Jordan-Sciutto. 2010. 'HIV-Associated
202 Neurocognitive Disorder: Pathogenesis and Therapeutic Opportunities', *Journal of*
203 *Neuroimmune Pharmacology*, 5: 294-309.
204 Mackelprang, R. D., A. Filali-Mouhim, B. Richardson, F. Lefebvre, E. Katabira, A. Ronald, G. Gray, K. W.
205 Cohen, N. R. Klatt, T. Pecor, C. Celum, M. J. McElrath, S. M. Hughes, F. Hladik, M. J. Cameron,
206 and J. R. Lingappa. 2023. 'Upregulation of IFN-stimulated genes persists beyond the transitory
207 broad immunologic changes of acute HIV-1 infection', *iScience*, 26: 106454.
208 Maddison, D. C., and F. Giorgini. 2015. 'The kynurenine pathway and neurodegenerative disease',
209 *Semin Cell Dev Biol*, 40: 134-41.
210 Malpass, K. 2011. 'Neurodegenerative disease: the kynurenine pathway--promising new targets and
211 therapies for neurodegenerative disease', *Nat Rev Neurol*, 7: 417.
212 Marodon, Gilles, David Warren, Michael C. Filomio, and David N. Posnett. 1999. 'Productive infection of
213 double-negative T cells with HIV in vivo', *Proceedings of the National*
214 *Academy of Sciences*, 96: 11958.
215 McGlasson, Sarah, Alexa Jury, Andrew Jackson, and David Hunt. 2015. 'Type I interferon dysregulation
216 and neurological disease', *Nature Reviews Neurology*, 11: 515-23.

217 Merimsky, Ofer, Irith Reider-Groswasser, Moshe Inbar, and Samario Chaitchik. 1990. 'Interferon-
218 related mental deterioration and behavioral changes in patients with renal cell carcinoma',
219 *European Journal of Cancer and Clinical Oncology*, 26: 596-600.
220 Merrill, J. E., Y. Koyanagi, J. Zack, L. Thomas, F. Martin, and I. S. Chen. 1992. 'Induction of interleukin-1
221 and tumor necrosis factor alpha in brain cultures by human immunodeficiency virus type 1',
222 *Journal of Virology*, 66: 2217.
223 Min, A. K., B. Javidfar, R. Missall, D. Doanman, M. Durens, S. S. Vil, Z. Masih, M. Graziani, A. Mordelt, S.
224 Marro, L. de Witte, B. K. Chen, T. H. Swartz, and S. Akbarian. 2023. 'HIV-1 infection of
225 genetically engineered iPSC-derived central nervous system-engrafted microglia in a humanized
226 mouse model', *bioRxiv*.
227 Mitrasinovic, Olivera M., Grace V. Perez, FeiFei Zhao, Yuen Ling Lee, Clara Poon, and Greer M. Murphy.
228 2001. 'Overexpression of Macrophage Colony-stimulating Factor Receptor on Microglial Cells
229 Induces an Inflammatory Response*', *Journal of Biological Chemistry*, 276: 30142-49.
230 Moretti, S., S. Virtuoso, L. Sernicola, S. Farcomeni, M. T. Maggiorella, and A. Borsetti. 2021. 'Advances
231 in SIV/SHIV Non-Human Primate Models of NeuroAIDS', *Pathogens*, 10.
232 Nasr, N., A. A. Alshehri, T. K. Wright, M. Shahid, B. M. Heiner, A. N. Harman, R. A. Botting, K. J. Helbig,
233 M. R. Beard, K. Suzuki, A. D. Kelleher, P. Hertzog, and A. L. Cunningham. 2017. 'Mechanism of
234 Interferon-Stimulated Gene Induction in HIV-1-Infected Macrophages', *J Virol*, 91.
235 Ormel, Paul R., Renata Vieira de Sá, Emma J. van Bodegraven, Henk Karst, Oliver Harschnitz, Marjolein
236 A. M. Sneeboer, Lill Eva Johansen, Roland E. van Dijk, Nicky Scheefhals, Amber Berdenis van
237 Berlekom, Eduardo Ribes Martínez, Sandra Kling, Harold D. MacGillavry, Leonard H. van den
238 Berg, René S. Kahn, Elly M. Hol, Lot D. de Witte, and R. Jeroen Pasterkamp. 2018. 'Microglia
239 innately develop within cerebral organoids', *Nature Communications*, 9: 4167.
240 Paolicelli, Rosa C., Giulia Bolasco, Francesca Pagani, Laura Maggi, Maria Scianni, Patrizia Panzanelli,
241 Maurizio Giustetto, Tiago Alves Ferreira, Eva Guiducci, Laura Dumas, Davide Ragozzino, and
242 Cornelius T. Gross. 2011. 'Synaptic Pruning by Microglia Is Necessary for Normal Brain
243 Development', *Science*, 333: 1456.
244 Paşca, Anca M., Steven A. Sloan, Laura E. Clarke, Yuan Tian, Christopher D. Makinson, Nina Huber, Chul
245 Hoon Kim, Jin-Young Park, Nancy A. O'Rourke, Khoa D. Nguyen, Stephen J. Smith, John R.
246 Huguenard, Daniel H. Geschwind, Ben A. Barres, and Sergiu P. Paşca. 2015. 'Functional cortical
247 neurons and astrocytes from human pluripotent stem cells in 3D culture', *Nature Methods*, 12:
248 671-78.
249 Pavol, M. A., C. A. Meyers, J. L. Rexer, A. D. Valentine, P. J. Mattis, and M. Talpaz. 1995. 'Pattern of
250 neurobehavioral deficits associated with interferon alfa therapy for leukemia', *Neurology*, 45:
251 947-50.
252 Peluso, Michael J., Victor Valcour, Nittaya Phanuphak, Jintanat Ananworanich, James L. K. Fletcher,
253 Thep Chalermchai, Shelly J. Krebs, Merlin L. Robb, Joanna Hellmuth, Magnus Gisslén, Henrik
254 Zetterberg, Serena Spudich, Rv Search Rv254Search, and Search Study Teams. 2017. 'Immediate
255 initiation of cART is associated with lower levels of cerebrospinal fluid YKL-40, a marker of
256 microglial activation, in HIV-1 infection', *AIDS (London, England)*, 31: 247-52.
257 Perrella, O., P. B. Carreiri, A. Perrella, C. Sbreglia, F. Gorga, D. Guarnaccia, and G. Tarantino. 2001.
258 'Transforming growth factor beta-1 and interferon-alpha in the AIDS dementia complex (ADC):
259 possible relationship with cerebral viral load?', *Eur Cytokine Netw*, 12: 51-5.

260 Phetsouphanh, Chansavath, David R. Darley, Daniel B. Wilson, Annett Howe, C. Mee Ling Munier,
261 Sheila K. Patel, Jennifer A. Juno, Louise M. Burrell, Stephen J. Kent, Gregory J. Dore, Anthony D.
262 Kelleher, and Gail V. Matthews. 2022. 'Immunological dysfunction persists for 8 months
263 following initial mild-to-moderate SARS-CoV-2 infection', *Nature Immunology*, 23: 210-16.
264 Platanias, Leonidas C. 2005. 'Mechanisms of type-I- and type-II-interferon-mediated signalling', *Nature*
265 *Reviews Immunology*, 5: 375-86.
266 Qian, Xuyu, Yijing Su, Christopher D. Adam, Andre U. Deutschmann, Sarshan R. Pather, Ethan M.
267 Goldberg, Kenong Su, Shiying Li, Lu Lu, Fadi Jacob, Phuong T. T. Nguyen, Sooyoung Huh, Ahmet
268 Hoke, Sarah E. Swinford-Jackson, Zhexing Wen, Xiaosong Gu, R. Christopher Pierce, Hao Wu,
269 Lisa A. Briand, H. Isaac Chen, John A. Wolf, Hongjun Song, and Guo-li Ming. 2020. 'Sliced Human
270 Cortical Organoids for Modeling Distinct Cortical Layer Formation', *Cell Stem Cell*, 26: 766-81.e9.
271 Quadrato, Giorgia, Tuan Nguyen, Evan Z. Macosko, John L. Sherwood, Sung Min Yang, Daniel R. Berger,
272 Natalie Maria, Jorg Scholvin, Melissa Goldman, Justin P. Kinney, Edward S. Boyden, Jeff W.
273 Lichtman, Ziv M. Williams, Steven A. McCarroll, and Paola Arlotta. 2017. 'Cell diversity and
274 network dynamics in photosensitive human brain organoids', *Nature*, 545: 48-53.
275 Rai, Mohammad A., Jason Hammonds, Mario Pujato, Christopher Mayhew, Krishna Roskin, and Paul
276 Spearman. 2020. 'Comparative analysis of human microglial models for studies of HIV
277 replication and pathogenesis', *Retrovirology*, 17: 35.
278 Raison, Charles L., Marina Demetrashvili, Lucile Capuron, and Andrew H. Miller. 2005.
279 'Neuropsychiatric Adverse Effects of Interferon-α', *CNS Drugs*, 19: 105-23.
280 Ramesh, Geeta, Andrew G. MacLean, and Mario T. Philipp. 2013. 'Cytokines and Chemokines at the
281 Crossroads of Neuroinflammation, Neurodegeneration, and Neuropathic Pain', *Mediators of*
282 *Inflammation*, 2013: 480739.
283 Rappaport, Jay, Jeymohan Joseph, Sidney Croul, Guillermo Alexander, Luis Del Valle, Shohreh Amini,
284 and Kamel Khalili. 1999. 'Molecular pathway involved in HIV-1-induced CNS pathology: role of
285 viral regulatory protein, Tat', *Journal of Leukocyte Biology*, 65: 458-65.
286 Rho, M. B., S. Wesselingh, J. D. Glass, J. C. McArthur, S. Choi, J. Griffin, and W. R. Tyor. 1995. 'A
287 Potential Role for Interferon-α in the Pathogenesis of HIV-Associated Dementia', *Brain,*
288 *Behavior, and Immunity*, 9: 366-77.
289 Roy, Ethan R., Gabriel Chiu, Sanming Li, Nicholas E. Propson, Rupa Kanchi, Baiping Wang, Cristian
290 Coarfa, Hui Zheng, and Wei Cao. 2022. 'Concerted type I interferon signaling in microglia and
291 neural cells promotes memory impairment associated with amyloid β plaques', *Immunity*, 55:
292 879-94.e6.
293 Roy, Ethan R., Baiping Wang, Ying-wooi Wan, Gabriel Chiu, Allysa Cole, Zhuoran Yin, Nicholas E.
294 Propson, Yin Xu, Joanna L. Jankowsky, Zhandong Liu, Virginia M. Y. Lee, John Q. Trojanowski,
295 Stephen D. Ginsberg, Oleg Butovsky, Hui Zheng, and Wei Cao. 2020. 'Type I interferon response
296 drives neuroinflammation and synapse loss in Alzheimer disease', *The Journal of Clinical*
297 *Investigation*, 130: 1912-30.
298 Ruhanya, Vurayai, Graeme B. Jacobs, Shalena Naidoo, Robert H. Paul, John A. Joska, Soraya Seedat,
299 George Nyandoro, Susan Engelbrecht, and Richard H. Glashoff. 2021. 'Impact of Plasma IP-
300 10/CXCL10 and RANTES/CCL5 Levels on Neurocognitive Function in HIV Treatment-Naive
301 Patients', *AIDS Research and Human Retroviruses*.
302 Ryan, Sean K., Michael V. Gonzalez, James P. Garifallou, Frederick C. Bennett, Kimberly S. Williams,
303 Nathaniel P. Sotuyo, Eugene Mironets, Kieona Cook, Hakon Hakonarson, Stewart A. Anderson,

304 and Kelly L. Jordan-Sciutto. 2020. 'Neuroinflammation and EIF2 Signaling Persist despite
305 Antiretroviral Treatment in an hiPSC Tri-culture Model of HIV Infection', *Stem Cell Reports*, 14:
306 703-16.
307 Sacktor, N., R. L. Skolasky, E. Seaberg, C. Munro, J. T. Becker, E. Martin, A. Ragin, A. Levine, and E.
308 Miller. 2016. 'Prevalence of HIV-associated neurocognitive disorders in the Multicenter AIDS
309 Cohort Study', *Neurology*, 86: 334-40.
310 Sacktor, Ned. 2018. 'Changing clinical phenotypes of HIV-associated neurocognitive disorders', *Journal*
311 *of NeuroVirology*, 24: 141-45.
312 Sanna, Pietro Paolo, Yu Fu, Eliezer Masliah, Celine Lefebvre, and Vez Repunte-Canonigo. 2021. 'Central
313 nervous system (CNS) transcriptomic correlates of human immunodeficiency virus (HIV) brain
314 RNA load in HIV-infected individuals', *Scientific Reports*, 11: 12176.
315 Schwarcz, R., and T. W. Stone. 2017. 'The kynurenine pathway and the brain: Challenges, controversies
316 and promises', *Neuropharmacology*, 112: 237-47.
317 Simioni, S., M. Cavassini, J. M. Annoni, A. Rimbault Abraham, I. Bourquin, V. Schiffer, A. Calmy, J. P.
318 Chave, E. Giacobini, B. Hirschel, and R. A. Du Pasquier. 2010. 'Cognitive dysfunction in HIV
319 patients despite long-standing suppression of viremia', *Aids*, 24: 1243-50.
320 Sloan, Steven A., Jimena Andersen, Anca M. Pașca, Fikri Birey, and Sergiu P. Pașca. 2018. 'Generation
321 and assembly of human brain region–specific three-dimensional cultures', *Nature Protocols*, 13:
322 2062-85.
323 Smith, Amy M., Hannah M. Gibbons, Robyn L. Oldfield, Peter M. Bergin, Edward W. Mee, Maurice A.
324 Curtis, Richard L. M. Faull, and Mike Dragunow. 2013. 'M-CSF increases proliferation and
325 phagocytosis while modulating receptor and transcription factor expression in adult human
326 microglia', *Journal of Neuroinflammation*, 10: 859.
327 Solomon, Isaac H., Sukrutha Chettimada, Vikas Misra, David R. Lorenz, Robert J. Gorelick, Benjamin B.
328 Gelman, Susan Morgello, and Dana Gabuzda. 2020. 'White Matter Abnormalities Linked to
329 Interferon, Stress Response, and Energy Metabolism Gene Expression Changes in Older HIV-
330 Positive Patients on Antiretroviral Therapy', *Molecular Neurobiology*, 57: 1115-30.
331 Song, Wilbur M., and Marco Colonna. 2018. 'The identity and function of microglia in
332 neurodegeneration', *Nature Immunology*, 19: 1048-58.
333 Sreeram, S., F. Ye, Y. Garcia-Mesa, K. Nguyen, A. El Sayed, K. Leskov, and J. Karn. 2022. 'The potential
334 role of HIV-1 latency in promoting neuroinflammation and HIV-1-associated neurocognitive
335 disorder', *Trends Immunol*, 43: 630-39.
336 Swingler, M., M. Donadoni, A. Bellizzi, S. Cakir, and I. K. Sariyer. 2023. 'iPSC-derived three-dimensional
337 brain organoid models and neurotropic viral infections', *J Neurovirol*, 29: 121-34.
338 Tang, Y., A. Chaillon, S. Gianella, L. M. Wong, D. Li, T. L. Simermeyer, M. Porrachia, C. Ignacio, B.
339 Woodworth, D. Zhong, J. Du, E. de la Parra Polina, J. Kirchherr, B. Allard, M. L. Clohosey, M.
340 Moeser, A. L. Sondgeroth, G. D. Whitehill, V. Singh, A. Dashti, D. M. Smith, J. J. Eron, K. J. Bar, A.
341 Chahroudi, S. B. Joseph, N. M. Archin, D. M. Margolis, and G. Jiang. 2023. 'Brain microglia serve
342 as a persistent HIV reservoir despite durable antiretroviral therapy', *J Clin Invest*, 133.
343 Valverde-Villegas, J. M., R. M. de Medeiros, J. H. Ellwanger, B. R. Santos, M. G. Melo, S. E. M. Almeida,
344 and J. A. B. Chies. 2018. 'High CXCL10/IP-10 levels are a hallmark in the clinical evolution of the
345 HIV infection', *Infect Genet Evol*, 57: 51-58.

346 van Marle, G., S. Henry, T. Todoruk, A. Sullivan, C. Silva, S. B. Rourke, J. Holden, J. C. McArthur, M. J.
347 Gill, and C. Power. 2004. 'Human immunodeficiency virus type 1 Nef protein mediates neural
348 cell death: a neurotoxic role for IP-10', *Virology*, 329: 302-18.
349 Vaughan-Jackson, Alun, Szymon Stodolak, Kourosh H. Ebrahimi, Cathy Browne, Paul K. Reardon,
350 Elisabete Pires, Javier Gilbert-Jaramillo, Sally A. Cowley, and William S. James. 2021.
351 'Differentiation of human induced pluripotent stem cells to authentic macrophages using a
352 defined, serum-free, open-source medium', *Stem Cell Reports*, 16: 1735-48.
353 Velasco, Silvia, Amanda J. Kedaigle, Sean K. Simmons, Allison Nash, Marina Rocha, Giorgia Quadrato,
354 Bruna Paulsen, Lan Nguyen, Xian Adiconis, Aviv Regev, Joshua Z. Levin, and Paola Arlotta. 2019.
355 'Individual brain organoids reproducibly form cell diversity of the human cerebral cortex',
356 *Nature*, 570: 523-27.
357 Vodyanik, Maxim A., James A. Thomson, and Igor I. Slukvin. 2006. 'Leukosialin (CD43) defines
358 hematopoietic progenitors in human embryonic stem cell differentiation cultures', *Blood*, 108:
359 2095-105.
360 Wei, Zhengyu, Brittany Bodnar, Ruo-Tong Zhao, Qianhao Xiao, Sami Saribas, Xu Wang, Wen-Zhe Ho,
361 and Wenhui Hu. 2023. 'Human iPSC-derived brain organoids: A 3D mini-brain model for
362 studying HIV infection', *Experimental Neurology*, 364: 114386.
363 Wichers, M. C., G. H. Koek, G. Robaeys, A. J. Praamstra, and M. Maes. 2005. 'Early increase in
364 vegetative symptoms predicts IFN-α-induced cognitive-depressive changes', *Psychological*
365 *Medicine*, 35: 433-41.
366 Wiley, C. A., R. A. Steinman, and Q. Wang. 2023. 'Innate immune activation without immune cell
367 infiltration in brains of murine models of Aicardi-Goutières Syndrome', *Brain Pathol*, 33:
368 e13118.
369 Woodburn, B. M., K. Kanchi, S. Zhou, N. Colaianni, S. B. Joseph, and R. Swanstrom. 2022.
370 'Characterization of Macrophage-Tropic HIV-1 Infection of Central Nervous System Cells and the
371 Influence of Inflammation', *J Virol*, 96: e0095722.
372 Xu, R., A. J. Boreland, X. Li, C. Erickson, M. Jin, C. Atkins, Z. P. Pang, B. P. Daniels, and P. Jiang. 2021.
373 'Developing human pluripotent stem cell-based cerebral organoids with a controllable microglia
374 ratio for modeling brain development and pathology', *Stem Cell Reports*, 16: 1923-37.
375 Yoon, Se-Jin, Lubayna S. Elahi, Anca M. Pașca, Rebecca M. Marton, Aaron Gordon, Omer Revah, Yuki
376 Miura, Elisabeth M. Walczak, Gwendolyn M. Holdgate, H. Christina Fan, John R. Huguenard,
377 Daniel H. Geschwind, and Sergiu P. Pașca. 2019. 'Reliability of human cortical organoid
378 generation', *Nature Methods*, 16: 75-78.
379 Yu, H., A. B. Rabson, M. Kaul, Y. Ron, and J. P. Dougherty. 1996. 'Inducible human immunodeficiency
380 virus type 1 packaging cell lines', *Journal of Virology*, 70: 4530-37.
381 Zou, Zhongcheng, Ashley Chastain, Susan Moir, Jennifer Ford, Kathryn Trandem, Elena Martinelli,
382 Claudia Cicala, Paul Crocker, James Arthos, and Peter D. Sun. 2011. 'Siglecs Facilitate HIV-1
383 Infection of Macrophages through Adhesion with Viral Sialic Acids', *PLoS One*, 6: e24559.
384

385

FIGURE LEGENDS

Figure 1: Human microglia are efficiently generated from induced pluripotent stem cells

(A) Representative brightfield images showing the induction of iPSCs to mesodermal yolk sac embryoid bodies (EB) and then to primitive microglia progenitor cells (PMPs) and microglia.

(B) Representative confocal images of PMPs expressing the yolk sac marker CD235 and the hematopoietic progenitor cell marker CD43 in the 03SF cell line.

(C) RT-qPCR analysis of *IBA1* and *P2RY12* mRNA expression in iPSCs and iPSC-derived microglia; n=3 cell lines (03SF, CD06, CD52); t test; data are presented as the mean ± SEM.

(D) Representative confocal images of microglia stained for the microglial markers IBA1, P2Y12, CX3CR1, TMEM119, and PU1 and costained with DAPI; n = 3 cell lines (03SF, CD06, CD52).

(E) Representative confocal image of a microglial cell displaying ramified morphology after 4 weeks of coculture with neurons.

(F) Representative confocal images of a 03SF cell line iPSC-derived microglial neuronal coculture stained for neurons (MAP2), synapses (SYN1), and microglia (IBA1). (F1 and F2) Orthogonal view of microglial (IBA1+) processes colocalized with neuronal dendrites (MAP2) and synapses (SYN1).

(G) RT-qPCR analysis of *CD4* and *CCR5* mRNA from iPSCs and microglia; n=3 cell lines (03SF, CD06, CD52); t test; data are presented as the mean ± SEM.

Figure 2: HIV-1-infected microglia exhibit productive infection, activation, and dysregulated cytokine/chemokine production

(A) RT-qPCR analysis of viral *gag/pol* mRNA after infection with HIV-1 JRFL in microglia monocultures; n=3 independent infections of 03SF line iPSC-derived microglia.

(B) ELISA analysis of secreted p24 in the culture supernatant of microglia infected with HIV-1 JR-FL reveals productive infection; n=3 independent infections of 03SF iPSC-derived microglia.

(C) RT-qPCR analysis of *IL1β, TNFα*, and *IL-6* mRNA at days 16 and 23 post infection with HIV-1 JRFL; n=3 independent infections of 03SF iPSC-derived microglia, t test; data are presented as the mean ± SEM.

(D) RT-qPCR analysis of *CCL2, CCL3*, and *CCL5* mRNA at days 16 and 23 post infection with HIV-1 JRFL; n=3 independent infections of 03SF iPSC-derived microglia.

(E) RT-qPCR analysis of *IBA1* and *P2RY12* mRNA at days 16 and 23 post infection with HIV-1 JRFL; n=3 independent infections of 03SF iPSC-derived microglia.

(F) Luminex cytokine/chemokine analysis of secreted M-CSF and IP-10/CXCL10 culture supernatant from HIV-1 JRFL-infected microglia; n=3 independent infections of 03SF microglia, two-way ANOVA; data are presented as the mean ± SEM.

(G) Representative confocal images of nucleocapsid protein p24 staining in HIV-1 JRFL-infected 03SF-derived microglia ($IBA1^+$).

Figure 3: HIV-1-infected microglia exhibit productive infection, activation, and dysregulated cytokine/chemokine production

(A) RT-qPCR analysis of viral *gag/pol* mRNA at days 9, 16, 23, and 30 post infection with HIV-1 JRFL and HIV-1 YU2; n=3 independent infections of CD06 iPSC-derived microglia. t test

(B) ELISA analysis of secreted p24 in the culture supernatant of microglia infected with HIV-1 JRFL and HIV-1 YU2 at days 9, 15, 21, and 27 reveals productive infection; n=3 independent infections of CD06 iPSC-derived microglia.

(C) RT-qPCR analysis of *IL1β* and *TNFα* mRNA at days 9, 16, 23, and 30 post infection with HIV-1 JRFL and HIV-1 YU2; n=3 independent infections of CD06 iPSC-derived microglia.

(D) RT-qPCR analysis of *CCL2* and *CCL3* mRNA at days 9, 16, 23, and 30 post infection with HIV-1 JRFL and HIV-1 YU2; n=3 independent infections of CD06 iPSC-derived microglia.

(E) RT-qPCR analysis of *IBA1* and *P2RY12* mRNA at days 9, 16, 23, and 30 post infection with HIV-1 JRFL and HIV-1 YU2; n=3 independent infections of CD06 iPSC-derived microglia.

Figure 4: HIV-1 causes enrichment of type I interferon signaling pathways and sustained interferon activation

(A) A volcano plot illustrating differentially expressed genes (DEGs) in HIV-1 JRFL-infected vs mock-infected microglia on day 16 post infection; n=3 independent infections of 03SF line iPSC-derived microglia.

(B) GSEA plot showing enrichment of IFNα-responsive genes in HIV-1 JRFL-infected vs mock-infected microglia on day 16 post infection (NES, normalized enrichment score; FDR, false discovery rate).

(C) Gene Ontology (GO) analysis of upregulated DEGs in HIV-1 JRFL vs mock-infected microglia on day 16 post infection; n=3 independent infections of 03SF microglia.

(D) Gene Ontology (GO) analysis of downregulated DEGs in HIV-1 JRFL vs mock-infected microglia on day 16 post infection; n=3 independent infections of 03SF microglia.

(E) A heatmap illustrating significant upregulation of interferon-stimulated genes in HIV-1-infected vs mock-infected microglia on day 16 post infection; n=3 independent infections of 03SF microglia.

(F) A heatmap illustrating SIGLEC gene expression in HIV-1-infected vs mock-infected microglia on day 16 post infection; n=3 independent infections of 03SF microglia.

(G) RT-qPCR analysis of *CXCL10*, *RSAD2*, *ISG15*, and *IDO1* mRNA from HIV-1 JRFL-infected vs mock-infected microglia at days 16 and 23 post infection; n = 3 independent infections of 03SF iPSC-derived microglia, t test; *$p < 0.05$, **$p < 0.01$, ***$p < 0.001$; data are presented as the mean ± SEM.

(H) RT-qPCR analysis of *CXCL10* and *RSAD2* mRNA from HIV-1 JRFL- and HIV-1 YU2-infected and mock-infected microglia at days 16 and 23 post infection; n = 4 independent infections of CD06 iPSC-derived microglia, t test; *$p < 0.05$, **$p < 0.01$, ***$p < 0.001$; data are presented as the mean ± SEM.

Figure 5: HIV-1-infected microglia incorporate into sliced cerebral organoids

(A) Representative confocal images of a day 144 organoid with neurons ($MAP2^+$), astrocytes ($GFAP^+$), and microglia ($IBA1^+$).

(B) Representative confocal images of day 144 organoids 14 days after the addition of HIV-1 JRFL-infected or mock-infected microglia; (B1) shows a high-magnification image of HIV-1-infected microglia from (B).

(C) High-magnification image of a single HIV-1-infected microglial cell within a sliced organoid.

(D) RT-qPCR of *gag/pol* mRNA from HIV-1 JRFL-infected or mock-infected microglia organoids on day 14; n=3 independent infections of 03SF microglia; one-tailed t test; ****P<0.001; error bars represent SEM.

(E) ELISA analysis of secreted p24 in culture supernatant from HIV-1 JRFL-infected or mock-infected microglia organoid day 14; n=3 independent infections of 03SF microglia; one-tailed t test; **p<0.01; data are presented as the mean ± SEM.

(F) RT-qPCR analysis of *ISG15*, *RSAD2*, *IFITM3*, *MX1*, *IFI44*, and *IFI27* mRNA from HIV-1 JRFL-infected or mock-infected microglia organoids on day 14; n=3 independent infections of 03SF microglia; one-tailed t test; *p < 0.05, **p < 0.01, ***p < 0.001; data are presented as the mean ± SEM.

Figure S1: Microglial RT-qPCR analysis

(A) RT-qPCR analysis of *IBA1* and *P2RY12* mRNA expression in iPSCs and iPSC-derived microglia; n=3 cell lines (03SF, CD06, CD52) and 3 biological replicates/line; t test; data are presented as the mean ± SEM.

(B) RT-qPCR analysis of *CD4* and *CCR5* mRNA expression in iPSCs and iPSC-derived microglia; n=3 cell lines (03SF, CD06, CD52) and 3 biological replicates/line; t test; data are presented as the mean ± SEM.

Figure S2: PCR analysis of 2-LTR circles

(A) A schematic representation of HIV-1 structure.

(B) A schematic representation of an HIV-1 2-LTR circle.

(C) PCR analysis of 2-LTR circles on day 4 post HIV-1 JRFL infection and mock infection.

Figure S3: RNA-seq analysis of HIV-1 JRFL- vs mock-infected 03SF microglia

(A) A PCA plot of RNA-seq data collected from HIV-1 JRFL-infected microglia vs mock-infected microglia on day 16; n=3 independent infections of 03SF microglia.

(B) A REVIGO treemap indicating major dysregulated pathways from gene ontology (GO) analysis of HIV-1 JRFL-infected microglia vs mock-infected microglia on day 16; n=3 independent infections of 03SF microglia.

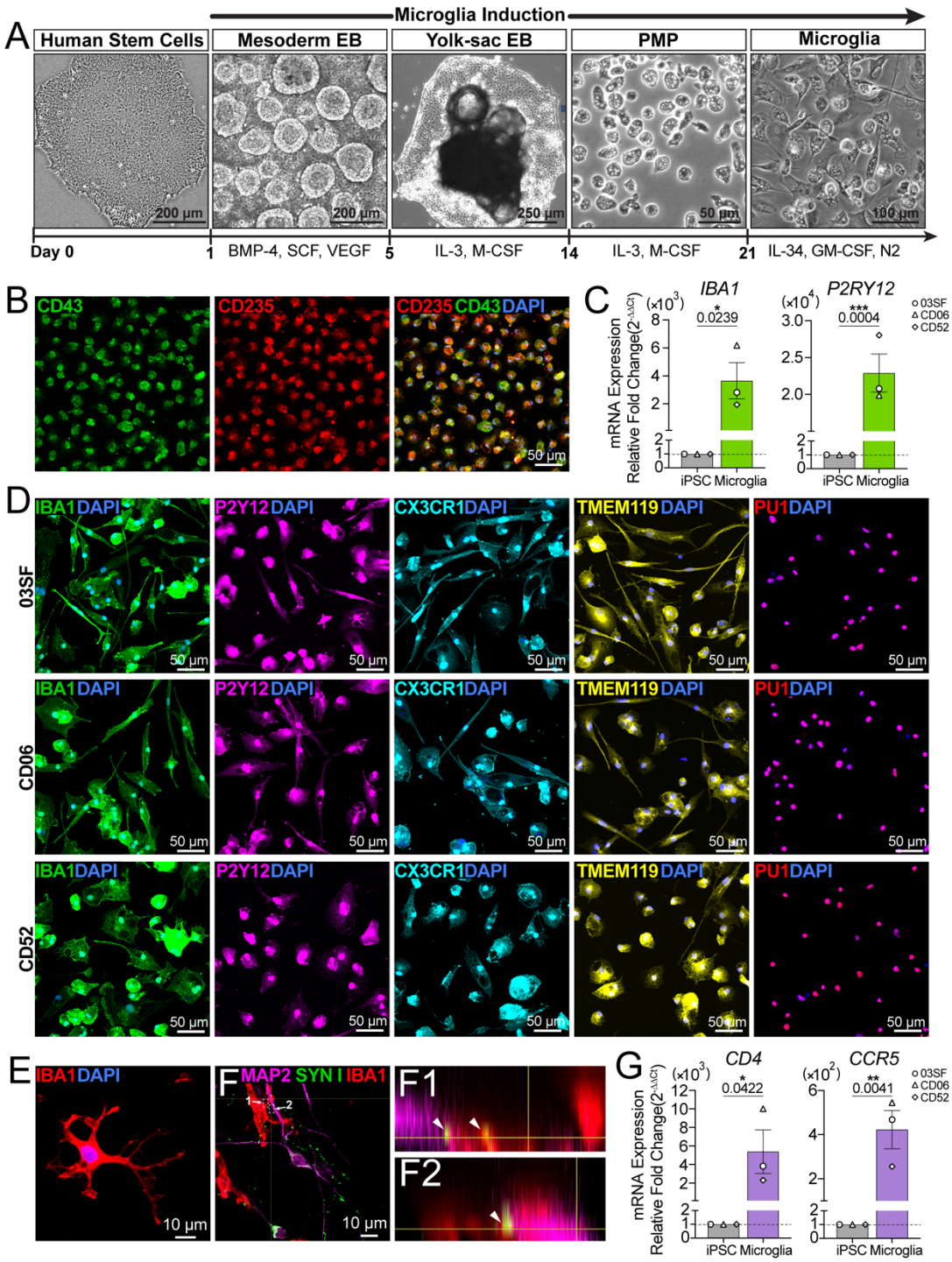
A
Microglia Induction
Human Stem Cells
Mesoderm EB
Yolk-sac EB
PMP
Microglia
200 µm
200 µm
250 µm
50 µm
100 µm
Day 0
1
BMP-4, SCF, VEGF
5
IL-3, M-CSF
14
IL-3, M-CSF
21
IL-34, GM-CSF, N2
B
CD43
CD235
CD235 CD43 DAPI
50 µm
C
IBA1
P2RY12
mRNA Expression Relative Fold Change(2^-ΔΔCt)
(×10^3)
(×10^4)
0.0239
0.0004
03SF
CD06
CD52
iPSC Microglia
iPSC Microglia
D
03SF
CD06
CD52
IBA1 DAPI
P2Y12 DAPI
CX3CR1 DAPI
TMEM119 DAPI
PU1 DAPI
50 µm
E
IBA1 DAPI
10 µm
F
MAP2 SYN I IBA1
10 µm
F1
F2
G
CD4
CCR5
mRNA Expression Relative Fold Change(2^-ΔΔCt)
(×10^3)
(×10^2)
0.0422
0.0041
03SF
CD06
CD52
iPSC Microglia
iPSC Microglia

Figure 1

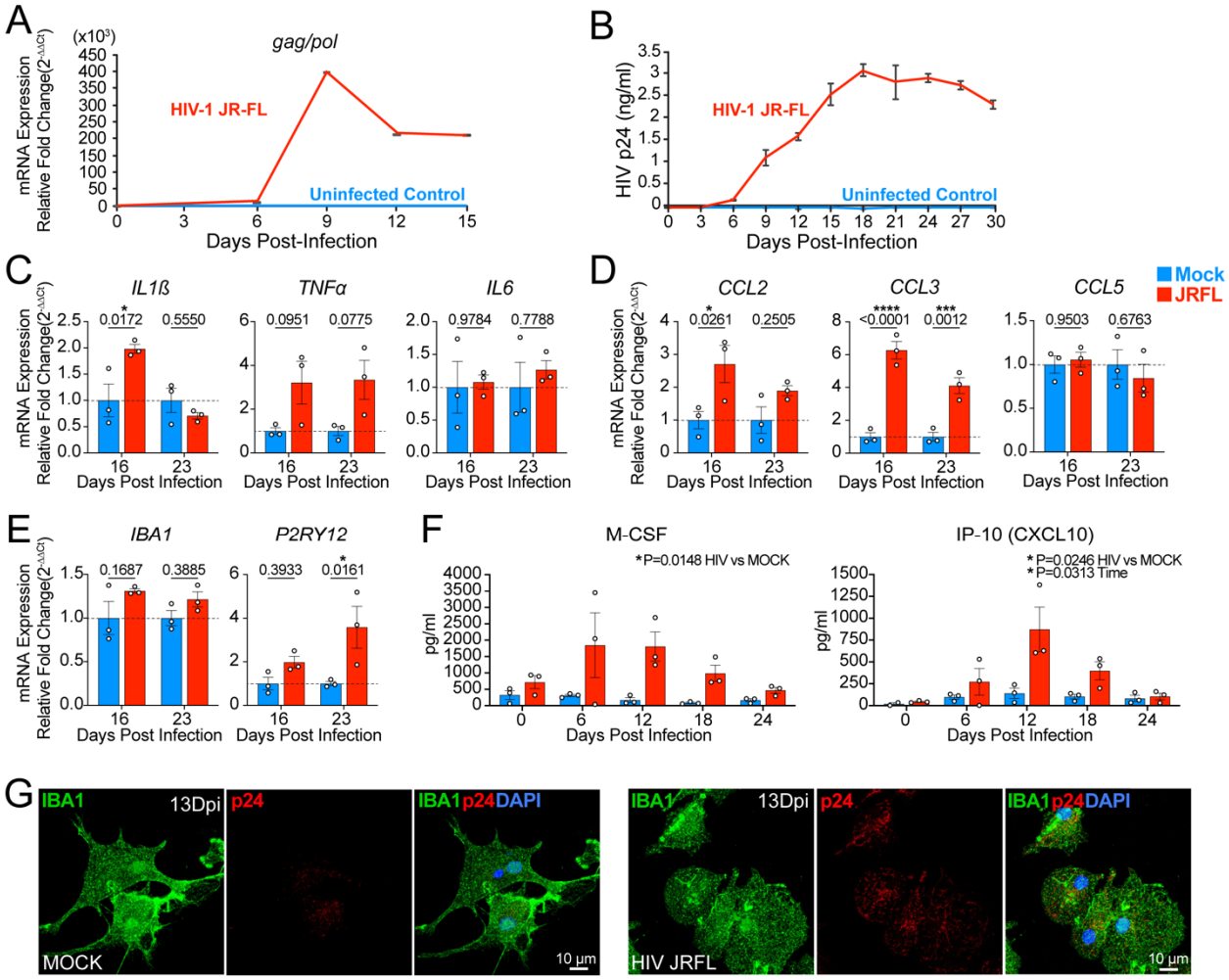
A
gag/pol
HIV-1 JR-FL
Uninfected Control
mRNA Expression Relative Fold Change(2^-ΔΔCt)
Days Post-Infection
B
HIV-1 JR-FL
Uninfected Control
HIV p24 (ng/ml)
Days Post-Infection
C
IL1ß
TNFα
IL6
0.0172
0.5550
0.0951
0.0775
0.9784
0.7788
Days Post Infection
D
CCL2
CCL3
CCL5
Mock
JRFL
0.0261
0.2505
<0.0001
0.0012
0.9503
0.6763
E
IBA1
P2RY12
0.1687
0.3885
0.3933
0.0161
F
M-CSF
*P=0.0148 HIV vs MOCK
IP-10 (CXCL10)
* P=0.0246 HIV vs MOCK
* P=0.0313 Time
pg/ml
G
IBA1
13Dpi
p24
IBA1p24DAPI
MOCK
HIV JRFL
10 µm

Figure 2

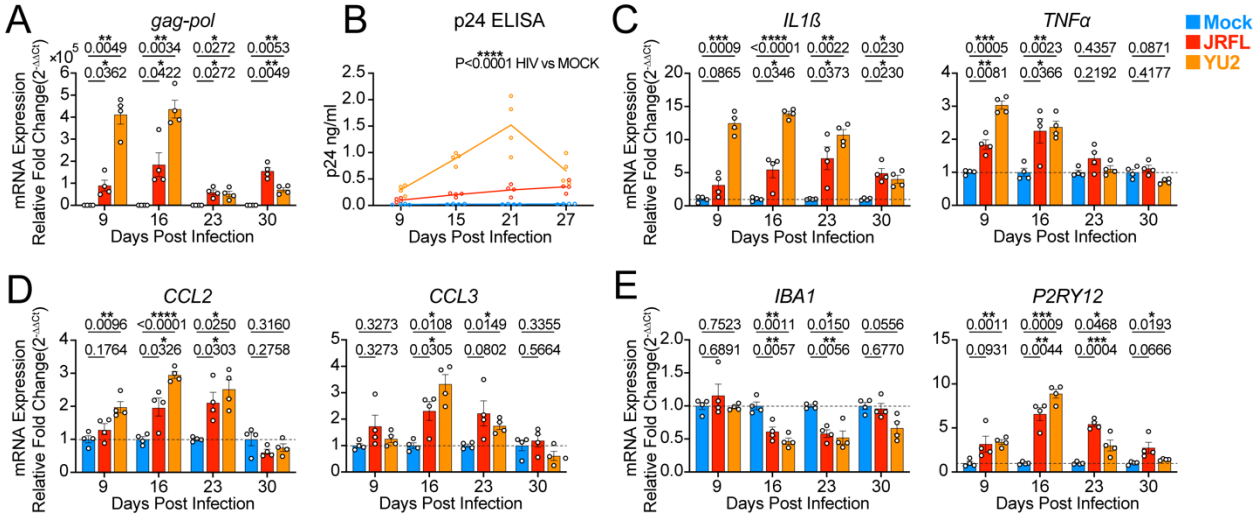
A
gag-pol
mRNA Expression
Relative Fold Change(2^-ΔΔCt)
Days Post Infection
B
p24 ELISA
P<0.0001 HIV vs MOCK
p24 ng/ml
Days Post Infection
C
IL1ß
TNFα
Mock
JRFL
YU2
D
CCL2
CCL3
E
IBA1
P2RY12

Figure 3

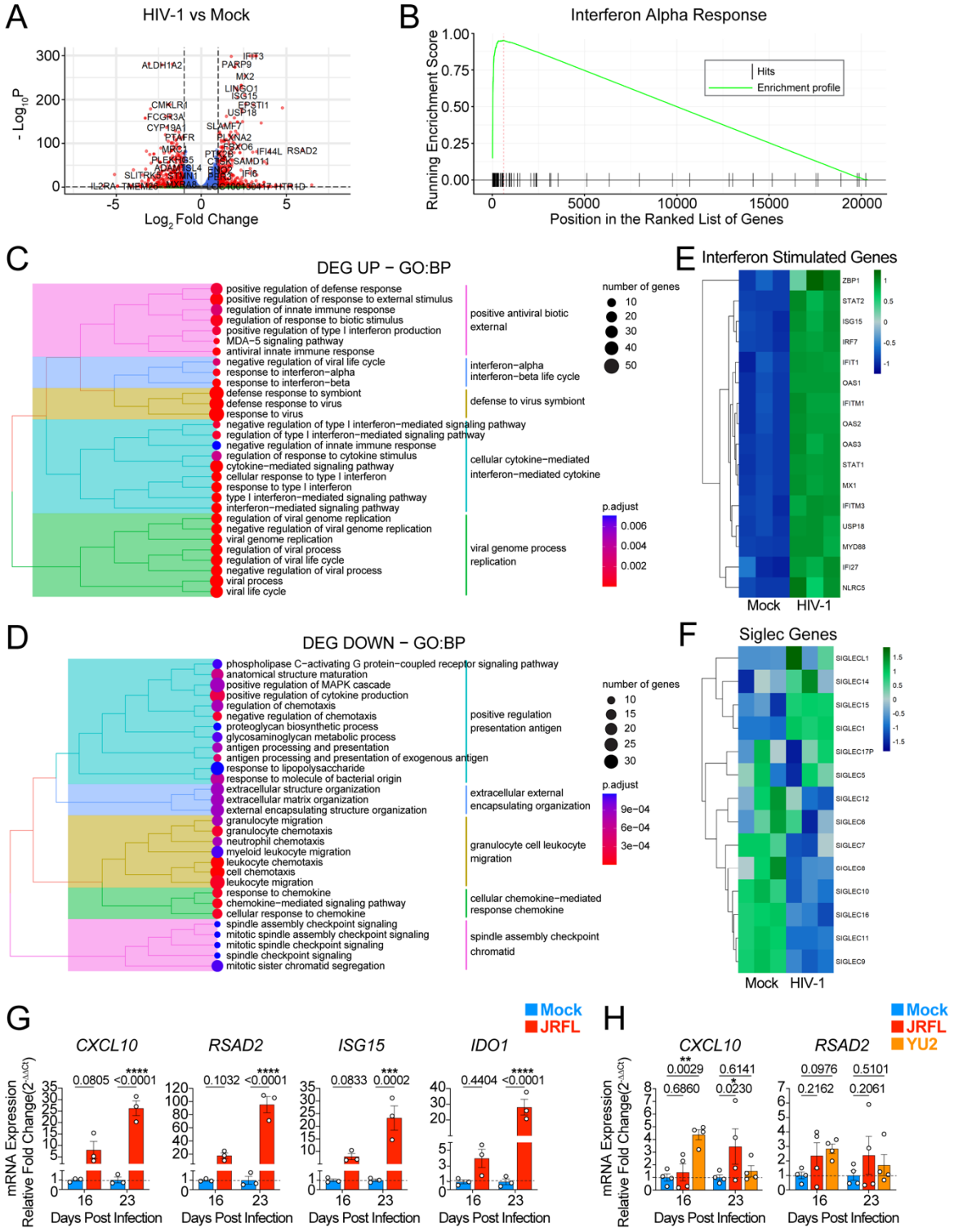
A
HIV-1 vs Mock
- Log10 P
Log2 Fold Change
B
Interferon Alpha Response
Running Enrichment Score
Hits
Enrichment profile
Position in the Ranked List of Genes
C
DEG UP − GO:BP
positive regulation of defense response
positive regulation of response to external stimulus
regulation of innate immune response
regulation of response to biotic stimulus
positive regulation of type I interferon production
MDA−5 signaling pathway
antiviral innate immune response
negative regulation of viral life cycle
response to interferon−alpha
response to interferon−beta
defense response to symbiont
defense response to virus
response to virus
negative regulation of type I interferon−mediated signaling pathway
regulation of type I interferon−mediated signaling pathway
negative regulation of innate immune response
regulation of response to cytokine stimulus
cytokine−mediated signaling pathway
cellular response to type I interferon
response to type I interferon
type I interferon−mediated signaling pathway
interferon−mediated signaling pathway
regulation of viral genome replication
negative regulation of viral genome replication
viral genome replication
regulation of viral process
regulation of viral life cycle
negative regulation of viral process
viral process
viral life cycle
positive antiviral biotic
external
interferon−alpha
interferon−beta life cycle
defense to virus symbiont
cellular cytokine−mediated
interferon−mediated cytokine
viral genome process
replication
number of genes
p.adjust
E
Interferon Stimulated Genes
ZBP1
STAT2
ISG15
IRF7
IFIT1
OAS1
IFITM1
OAS2
OAS3
STAT1
MX1
IFITM3
USP18
MYD88
IFI27
NLRC5
Mock
HIV-1
D
DEG DOWN − GO:BP
phospholipase C−activating G protein−coupled receptor signaling pathway
anatomical structure maturation
positive regulation of MAPK cascade
positive regulation of cytokine production
regulation of chemotaxis
negative regulation of chemotaxis
proteoglycan biosynthetic process
glycosaminoglycan metabolic process
antigen processing and presentation
antigen processing and presentation of exogenous antigen
response to lipopolysaccharide
response to molecule of bacterial origin
extracellular structure organization
extracellular matrix organization
external encapsulating structure organization
granulocyte migration
granulocyte chemotaxis
neutrophil chemotaxis
myeloid leukocyte migration
leukocyte chemotaxis
cell chemotaxis
leukocyte migration
response to chemokine
chemokine−mediated signaling pathway
cellular response to chemokine
spindle assembly checkpoint signaling
mitotic spindle assembly checkpoint signaling
mitotic spindle checkpoint signaling
spindle checkpoint signaling
mitotic sister chromatid segregation
positive regulation
presentation antigen
extracellular external
encapsulating organization
granulocyte cell leukocyte
migration
cellular chemokine−mediated
response chemokine
spindle assembly checkpoint
chromatid
number of genes
p.adjust
F
Siglec Genes
SIGLECL1
SIGLEC14
SIGLEC15
SIGLEC1
SIGLEC17P
SIGLEC5
SIGLEC12
SIGLEC6
SIGLEC7
SIGLEC8
SIGLEC10
SIGLEC16
SIGLEC11
SIGLEC9
Mock
HIV-1
G
Mock
JRFL
CXCL10
RSAD2
ISG15
IDO1
mRNA Expression
Relative Fold Change(2^-ΔΔCt)
Days Post Infection
H
Mock
JRFL
YU2
CXCL10
RSAD2
mRNA Expression
Relative Fold Change(2^-ΔΔCt)
Days Post Infection

Figure 4

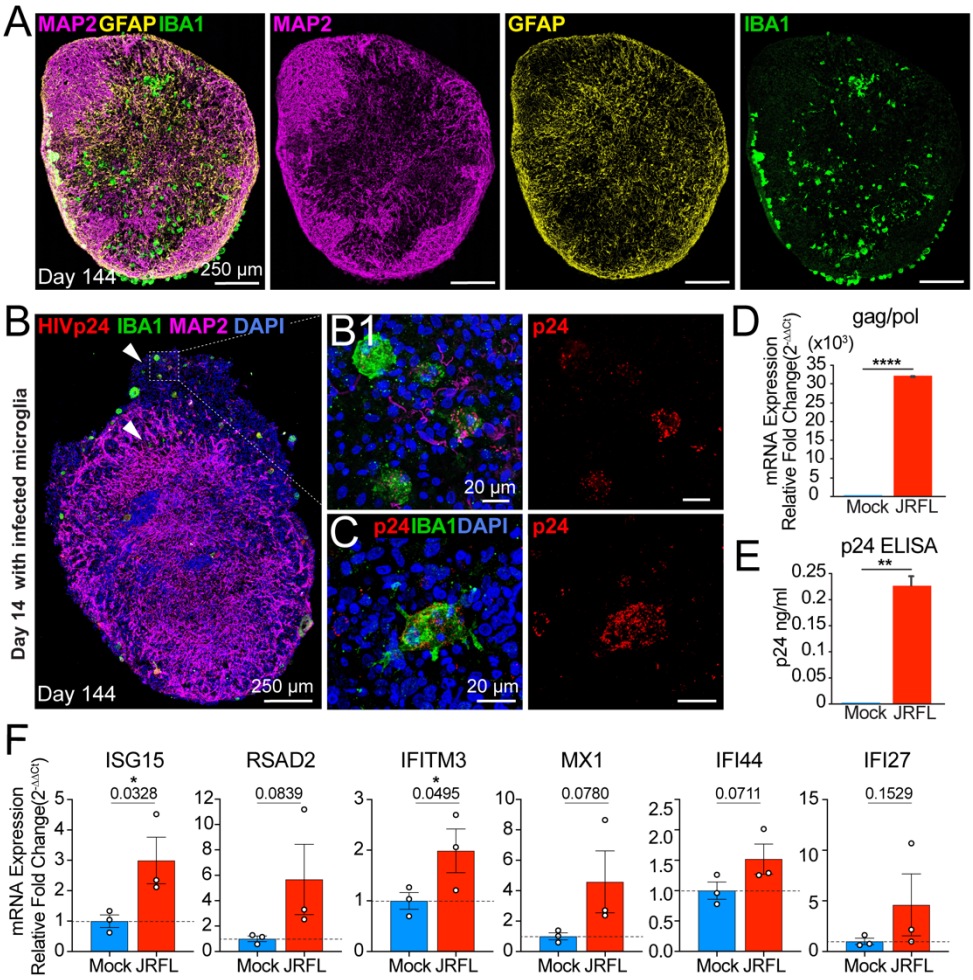
A
MAP2 GFAP IBA1
MAP2
GFAP
IBA1
Day 144
250 µm
B
HIV p24 IBA1 MAP2 DAPI
Day 14 with infected microglia
Day 144
250 µm
B1
p24
20 µm
C
p24 IBA1 DAPI
p24
20 µm
D
gag/pol
(x10³)
mRNA Expression Relative Fold Change(2^-ΔΔCt)
****
Mock JRFL
E
p24 ELISA
**
p24 ng/ml
Mock JRFL
F
ISG15
RSAD2
IFITM3
MX1
IFI44
IFI27
mRNA Expression Relative Fold Change(2^-ΔΔCt)
0.0328
0.0839
0.0495
0.0780
0.0711
0.1529
Mock JRFL

Figure 5

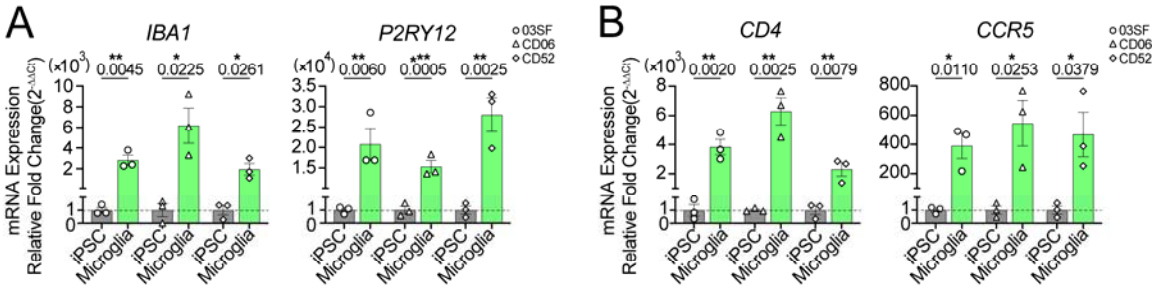

Supplemental Figure 1

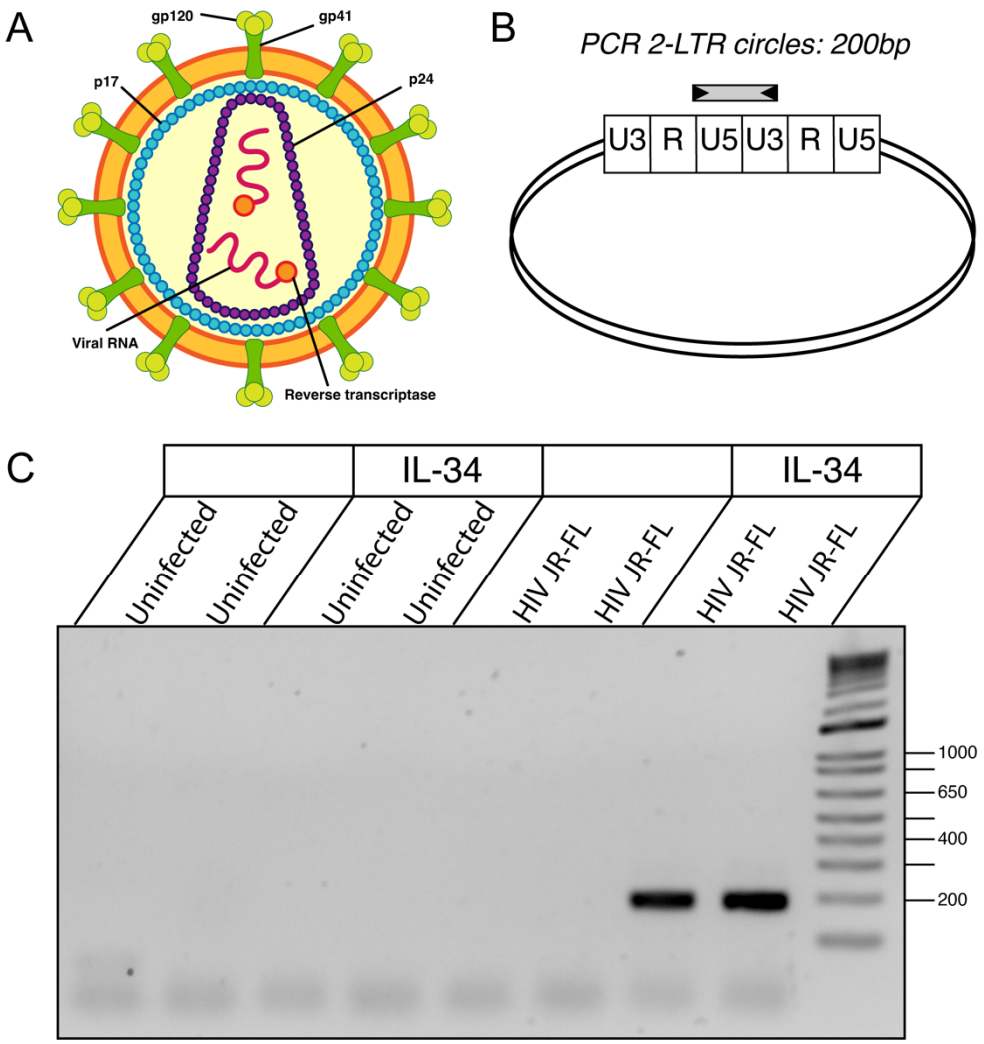

Supplemental Figure 2

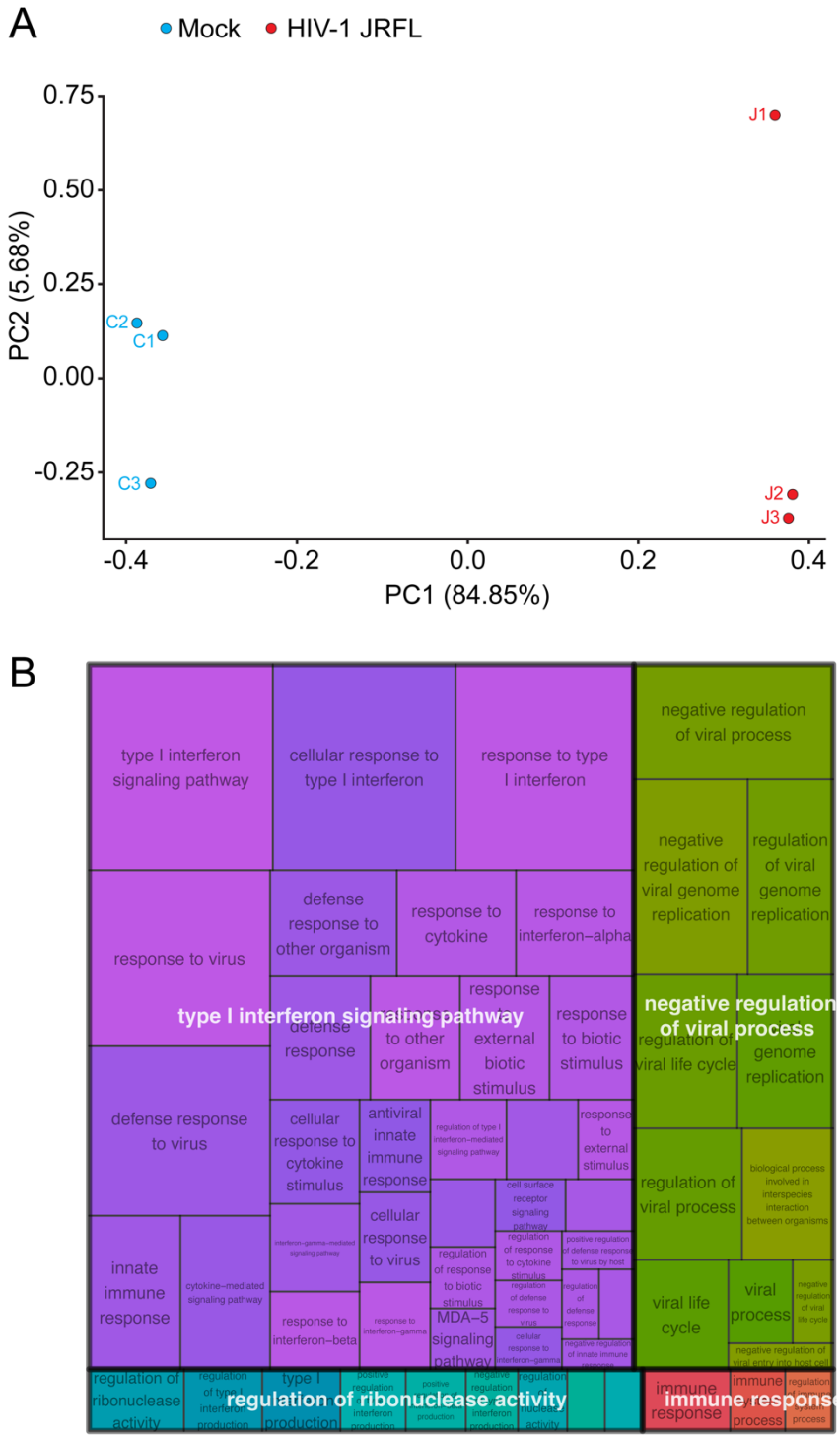

Supplemental Figure 3